The Asteroidal Population in the Hecuba Gap. Part II: Origin of the resonant asteroids

F. Roig

Instituto Astronômico e Geofísico, Universidade de São Paulo.

Av. Miguel Stefano 4200, (04301-904) São Paulo, SP, Brasil.

D. Nesvorný

Department of Space Studies, Southwest Research Institute.

1050 Walnut St., Suite 426, Boulder, CO 80302, USA

S. Ferraz-Mello

and

T.A. Michtchenko

Instituto Astronômico e Geofísico, Universidade de São Paulo

Av. Miguel Stefano 4200, (04301-904) São Paulo, SP, Brasil.

1. Introduction

This paper is the continuation of our work about the population of asteroids in the Hecuba gap. In our previous paper (Roig et al. 2001), hereinafter RNF-I, we studied the dynamical characteristics of the real asteroids in the 2:1 resonance with Jupiter. We identified 61 resonant asteroids known at April 2001, both numbered and unnumbered multi-oppositional, and divided them in three sub-populations: (i) stable objects, that are able to survive in the resonance for more than 500 Myr, (ii) marginally unstable, with typical lifetimes between 100 and 500 Myr, and (iii) unstable objects, with lifetimes smaller than 100 Myr (in most cases much smaller). The main members of the stable and marginally unstable populations are the asteroids (3789) Zhongguo and (11362) Griqua, respectively. Then, throughout this paper we will usually refer to these two populations simply as "the Zhongguos" and "the Griquas".

In RNF-I we have shown that the Zhongguos are about 30 asteroids located in the most stable region inside the 2:1 resonance, where they would be able to survive over the age of the Solar System. We have also discussed the role of Yarkovsky effect and of mutual scattering in enhancing the chaotic diffusion in this region, concluding that these processes do not affect significantly the long term stability of the Zhongguos. Then, the open problem is to determine if these objects have actually been in the resonance from the very primordial times, or if they arrived to their

present location in more recent times. As we discussed in RNF-I, the main argument against the primordiality of these resonant asteroids in the resonance is their steep size distribution and their rather small sizes (less than 20 km in diameter).

We have also shown in RNF-I that there is a possible dynamical link between the Griquas and the Zhongguos, supported by the natural chaotic diffusion in the resonant phase space. Concerning the unstable population, their members lie in the most unstable regions of the resonance, and we concluded that such asteroids should be continuously resupplied from outside the resonance in order to keep the population in steady state, as we presently observe it.

However, in RNF-I we did not do a detailed analysis and discussion of the specific mechanisms that could "inject" asteroids in the resonance, both in stable or unstable regions. The aim of this paper is to complete this analysis, presenting the main outlines of the most interesting alternatives. We do not intend to draw definitive conclusions about the origin of the resonant asteroids in the Hecuba gap, but rather to provide the necessary evidence that could allow to either support or discard any of these alternatives.

The mechanisms we will study here are basically three: (i) dynamical diffusion at the left side of the Hecuba gap (Sect. 2), (ii) resonant capture due to planetary migration (Sect. 3), and (iii) breakup of Themis and formation of Themis family (Sect. 4). In Sect. 2, we will also discuss the role of different sources of diffusion, like weak mean motion resonances, Yarkovsky effect, and mutual scattering. Most of the definitions and techniques applied in this section were already described in detail in RNF-I, and we will avoid to repeat their description here. Then, we will frequently refer the reader to that paper. Finally, Sect. 5 is devoted to the conclusions.

2. Diffusion in the neighborhood of the Hecuba gap

If we are looking for a reservoir of asteroids able to supply or resupply the population of resonant objects at the 2:1 resonance, then we have to look first at the left side of the resonance. The large density of background asteroids observed there is even enhanced by the presence of Themis family, which accounts for some 2000 asteroids. Moreover, the asteroidal density in the region shows a clear cutoff at the border of the 2:1 resonance, which means that a lot of asteroids lie very close to the separatrix and could be able to be injected somehow in the resonance. We will discuss in the following, how could this injection be favored by the chaotic diffusion at the left side of the Hecuba gap.

The first step was to mount a map of the diffusive structure near the separatrix of the 2:1 resonance. This map is shown in Fig. 1. The darker areas correspond to regions where the motion is very stable, while the lighter ones are associated to regions of strong chaos. The map was mounted by integrating a grid of 10,000 particles, regularly distributed in the a, e space. The initial angles were such that $\sigma = 2\lambda_{\rm J} - 2\lambda - \varpi = 0$, $\varpi - \varpi_{\rm J} = 0$ and $\Omega - \Omega_{\rm J} = 0$, and the model considered

perturbations of four major planets[1] . The chaoticity of each initial condition has been quantified by counting the number of peaks in the 1 Myr FFT spectrum of the semi-major axis, and this quantity was translated to a gray-scale.

This map of spectral numbers (Michtchenko and Ferraz-Mello, 2001) allowed to obtain a detailed portrait of the phase space with a relatively low computational cost. Several features can be appreciated in Fig. 1. At the upper right corner there is a huge region of chaos corresponding to the 2:1 resonant space. The "spot " of almost regularity in the middle of that region corresponds to the place where the Zhongguos are located. The border of the resonance is also quite well defined. Outside the resonance, we observe a complex web of weak mean motion resonances (MMRs), which appear as inclined stripes of instability. Most of these are three-body MMRs (Nesvorný and Morbidelli, 1998) involving the orbital periods of Jupiter and Saturn, and some of them are indicated at the bottom of the plot. The dominant ones are the 5:–2:–2 and 7:–2:–3 resonances[2]. Other weaker MMRs, as the stripes in each side of the 5:–2:–2 resonance, corresponds to combinations of the three-body MMR itself with the frequency of the 5:2 Great Inequality between Jupiter and Saturn. At high eccentricities ($e > 0.3$) several narrow MMRs overlap and generate the rather chaotic region observed at the upper left corner of the plot.

The role of these weak resonances is to enhance the chaotic diffusion in the (otherwise stable) neighborhood of the Hecuba gap. An asteroid captured in such resonances will randomly walk along it, being able to excite its eccentricity. In the inner main belt, this mechanism has been proven to be responsible of re-supplying the population of Mars-crossers (Morbidelli and Nesvorný, 1999), and of enhancing the proper element's dispersion of the Flora family (Nesvorný et al., 2001). An interesting feature observed in Fig. 1 is that some weak MMRs touch the border of the 2:1 resonance at a certain eccentricity. In the following, we will discuss whether or not these regions of contact could behave as "gates", allowing an asteroid captured in a narrow MMR to jump inside the 2:1 resonance after exciting its eccentricity.

2.1. Weak mean motion resonances

In order to analyze the efficiency of weak MMRs to inject asteroids in the 2:1 resonance, we performed a simulation of 300 test particles and studied their chaotic diffusion in the proper elements' space. We used the symplectic integrator Swift (Levison and Duncan, 1994), with a time step of 0.05 yr, and taking into account perturbation of four major planets. The simulation spanned 200 Myr. The initial conditions of the test particles were chosen as follows: the eccentricity was

[1] As usual, λ, ϖ and Ω represent the mean, perihelion and node longitudes, respectively, and the index J refers to Jupiter

[2] A three-body resonance of the form $k : -l : -m$ corresponds to a combination of frequencies $kn_{\rm J} - ln_{\rm S} - mn_{\rm A} \simeq 0$, where n refers to the mean motion of the bodies involved.

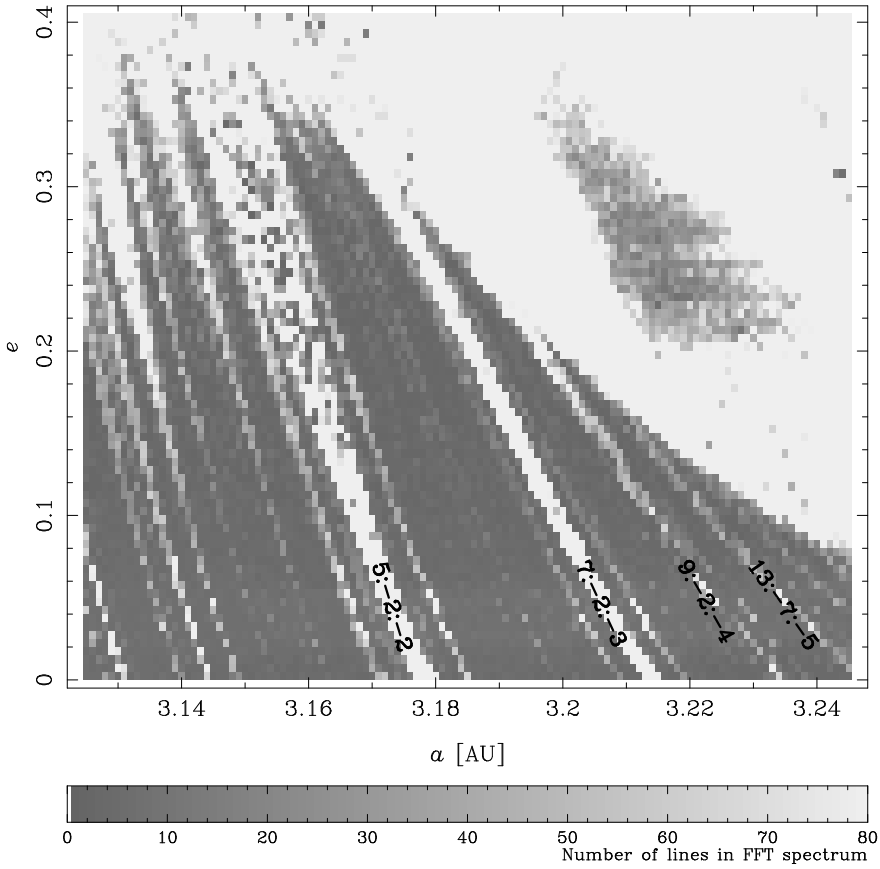

Fig. 1.— Map of spectral numbers (number of peaks in the FFT spectrum) for the left side of the Hecuba gap. The darkest regions are the most stable. The gray-scale is truncated at 80 peaks.

equally spaced in the range $0.05 \leq e \leq 0.4$, $\Delta e = 0.05$; the semi-major axis was also equally spaced in the range $a_{\rm min} \leq a \leq a_{\rm max}$, $\Delta a = 0.003$ AU, where $a_{\rm min}, a_{\rm max}$ depend on the initial eccentricity and varied between 3.10–3.15 and 3.24–3.27 AU, respectively. The remaining elements were chosen such that $\sigma = 0$, $\varpi - \varpi_{\rm J} = 0$, $I = 5°$, and Ω randomly distributed between 0 and 2π. We further divided these initial condition into two sub-sets:

- Set #1 corresponds to 200 initial conditions started the simulation outside the 2:1 resonance.
- Set #2 corresponds to 100 initial conditions that were in the resonance from the very beginning of the simulation (this was verified by looking at the average a and the behavior of σ).

From the results of this simulation, we computed time series of the proper elements a_p, e_p, I_p for each particle. For the particles of Set #1, proper elements were defined as the running averages of a, e, I over 10 Myr, and were sampled every 0.1 Myr. For the particles of Set #2, we followed the same procedure applied in RNF-I, and defined proper elements as the running minima of a and maxima of e, I, also over 10 Myr with 0.1 Myr sampling. It is worth noting that this last definition of proper elements (maxima/minima) can also be applied to the particles of Set #1. In such case, the maximum of the eccentricity has a particular meaning, because it is associated to the condition $\varpi - \varpi_{\rm J} = 0$. This latter set of proper elements are usually referred to as *resonant proper elements*, because they better describe the position of the asteroids with respect to the separatrix of the 2:1 resonance (Morbidelli et al., 1995). Although for Set #1 the averages normally provide proper elements of better quality, we will eventually use at times the maxima/minima to point out some particular dynamical features.

The typical evolution of the particles of Set #1 in the space of proper elements is shown in Fig. 2. In this figure, we plot the averaged values of a and e (sampled every 0.1 Myr) for all particles with initial conditions between $0.2 \leq e \leq 0.4$. It is worth noting that the initial conditions are related to a maximum of e, so the corresponding averaged eccentricities are shifted down by some 0.05. In Fig. 2 we also indicate the approximate location of some MMRs (vertical full lines), and also the curves corresponding to three different values of the invariant

$$N = \sqrt{a}\left(-2 + \sqrt{1-e^2}\cos I\right) \tag{1}$$

which is related to the 2:1 resonance (dashed lines marked N_i).

As we expected, the particles captured in MMRs show diffusive paths in e_p along these resonances. By far, the dominant resonance is 5:–2:–2. These particles also show a significant diffusion in a_p, although it is mostly limited to the width of each MMR. The diffusion in a_p is mainly due to the proper oscillations inside the MMRs and it is larger for larger e_p, because the resonance width increases with eccentricity. However, these proper oscillations have a superimposed forced oscillation, which is induced by the proximity to the 2:1 resonance. This is clearly noted in Fig. 2, where the diffusive paths in a_p are always aligned with the lines of $N = $ const. The particles that are not captured in the narrow MMRs can be identified as the tiny dashes in Fig. 2, mainly at

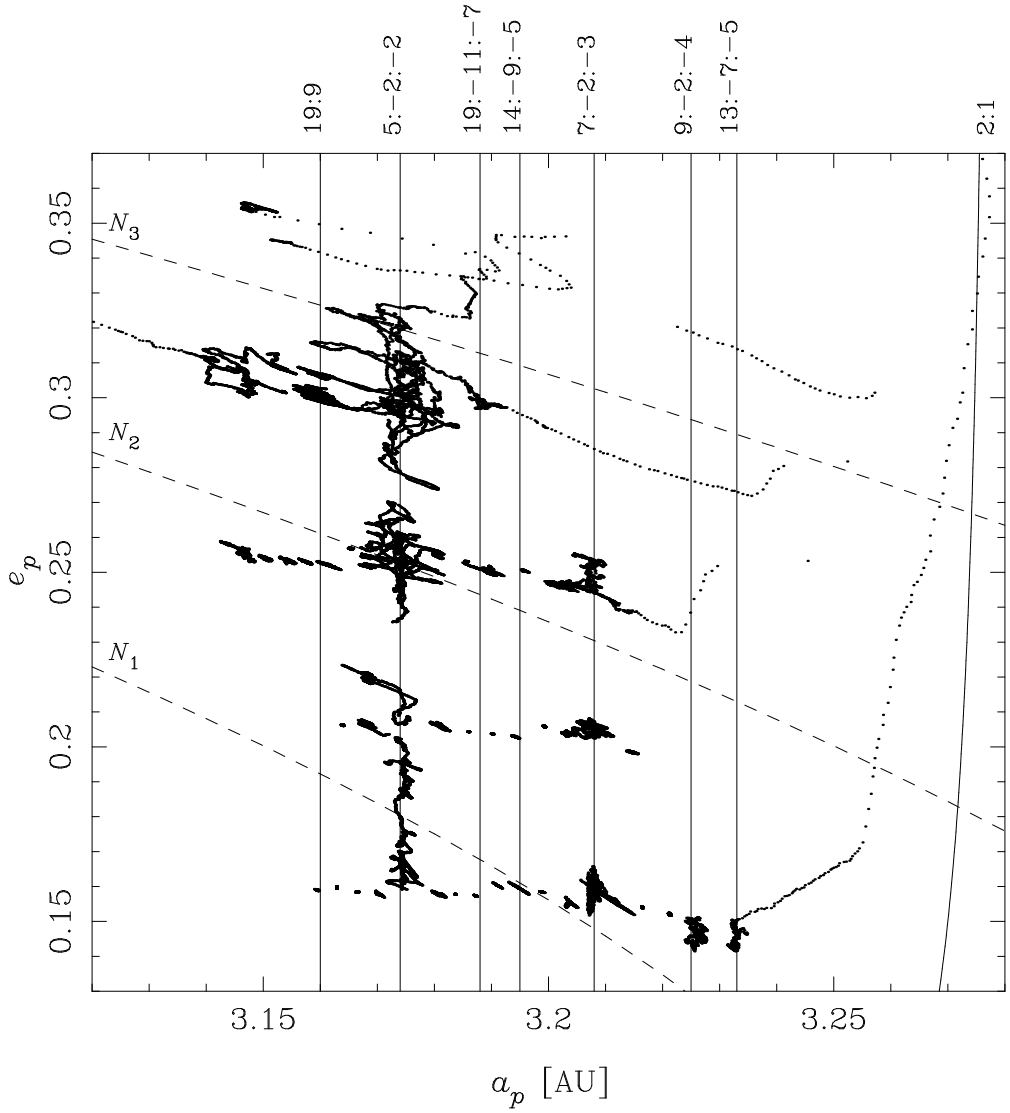

Fig. 2.— The evolution in the proper elements' space of the test particles in Set #1. Only the particles with initial $e \geq 0.2$ are shown. Proper elements are defined as averages over 10 Myr and are sampled every 0.1 Myr. Note that the average eccentricity is shifted down about 0.05 with respect to the initial eccentricity. The location of some MMRs resonance is indicated by full vertical lines, trucated at the approximate border of the 2:1 resonance. Dashed lines correspond to values of the invariant Eq. (1).

$e_p = 0.15$ and 0.20. No significant diffusion is observed in these cases, at least in the time scale of our simulation.

But for our purposes, the most interesting feature observed in Fig. 2 concerns the particles that went injected in the 2:1 resonance. We observe three clear examples at $e_p = 0.15$, 0.25 and 0.30, respectively, but a larger number of injections occurred also at $e_p = 0.35$. These injections happened precisely at the "gates" mentioned above, where the weak MMRs touch the 2:1 resonance border. In Fig. 3 we present the typical behavior of two of these injected particles: one of them had initially $e = 0.20$ (upper panels) and the other $e = 0.30$ (lower panels). For the sake of comparison, we also show in each case the behavior of a neighboring initial condition that was not injected during the simulation (dotted curves). The first case correspond to a particle that started the simulation inside the 13:–7:–5 resonance. The particle chaoticaly evolved there for about 100 Myr until it was pushed to enter the 2:1 resonance. The second case is a particle that started the simulation at the 7:–2:–3 resonance. Even being a stronger resonance, the particle spent more than 100 Myr in it before becoming thrown to the 2:1 resonance. This seems to indicate that the typical diffusion in e_p along the weak MMRs is not actually too large, and opens the question about the efficiency of this mechanism to excite the eccentricities and inject asteroids in the 2:1 resonance. In fact, the examples shown in Fig. 3 were quite lucky (or unlucky) particles, because they started the simulation not only at a weak MMR but also very close to the 2:1 resonance border.

Back to Fig. 2, the apparently large diffusive paths observed at the 5:–2:–2 resonance, for example between $0.15 \leq e_p \leq 0.22$, come in fact from the combined effect of two or more different particles, some of them diffusing upwards from a lower e_p while other diffusing downwards from a higher e_p. In spite of the quite enhanced diffusion at this resonance, it is difficult to imagine how could a particle at $e_p \simeq 0.15$ (for example, a typical Themis family member) be able to excite its eccentricity to much larger values in a time-scale shorter than the age of the Solar System. The dynamics of Themis family members is of the upmost importance, because this family concentrates a large fraction of the asteroidal population at the left side of the 2:1 resonance, and could be the most important reservoir of potential 2:1 resonant objects.

To better quantify the actual diffusion induced by the narrow MMRs at the left side of the Hecuba gap, we computed the diffusion parameters for each proper element, following the same procedure described in RNF-I. In short, given a proper element E, we introduced two different definitions for these parameters: the first one is simply the standard deviation σ_E of the proper element over a given time interval (do not mistake with the critical argument σ); the second is the slope β_E of the linear best-fit for the time series of the proper element. Figure 4 shows the values of $\sigma_a, \sigma_e, \sigma_I$ over 200 Myr, for the initial conditions of Set #1 with $e \leq 0.3$. We can see a correlation between the three quantities, which is related to the evolution at weak MMRs. The initial conditions with $e = 0.4$ were excluded from the plot because they evolve in a regime of overlap of MMRs, and their behavior is totally different from that of the lower e particles, as we will discuss later.

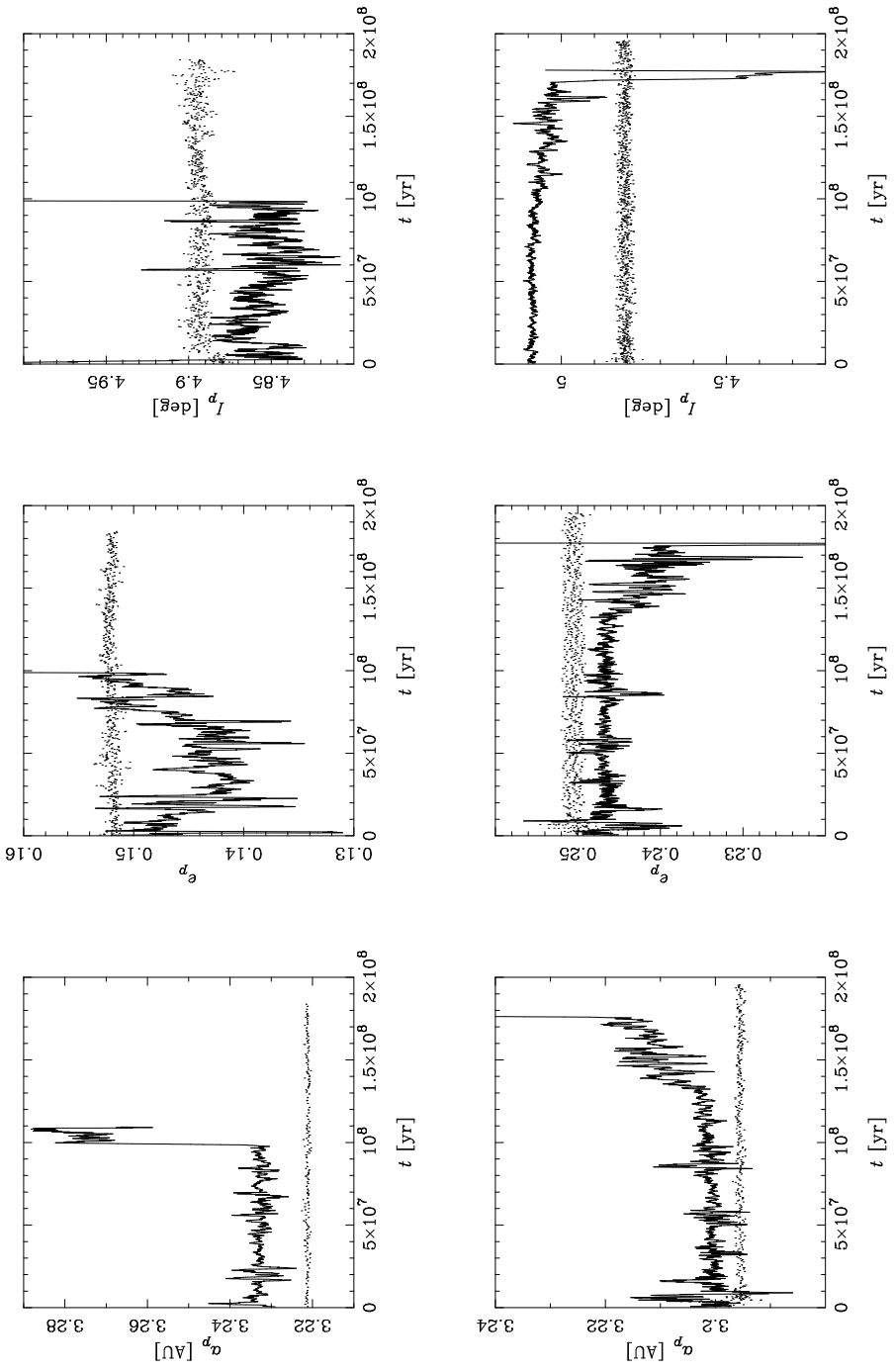

Fig. 3.— Two examples of the evolution of proper elements of particles injected in the 2:1 resonance during our simulation (full lines), and neighboring particles not injected (dotted lines). The upper panels correspond to initial conditions at $e = 0.2$ and the bottom ones, correspond to initial conditions at $e = 0.3$. At variance with Fig. 2, the proper elements shown here are averages over 1 Myr.

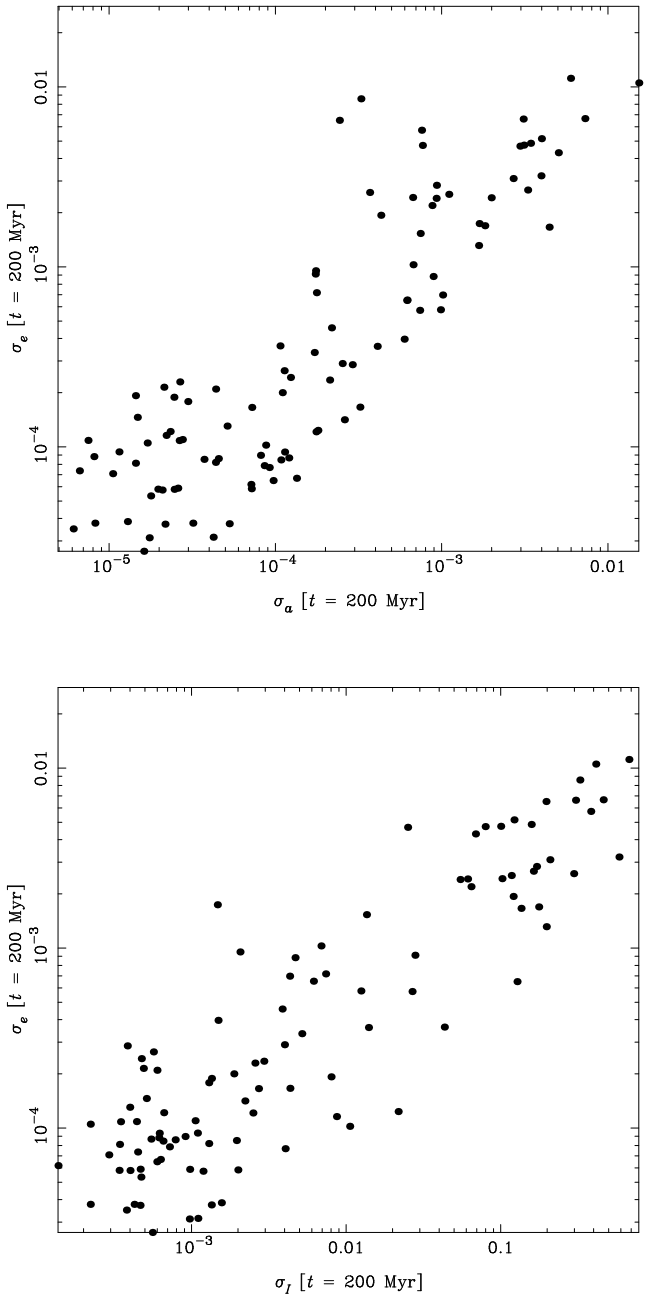

Fig. 4.— Diffusion parameters (standard deviations of proper elements over 200 Myr) for the test particles of Set #1. We are not showing the particles with initial $e = 0.4$. The correlation between the parameters is related to the chaotic diffusion inside the weak MMRs. Units are AU for σ_a, and deg for σ_I.

In Fig. 4 the large values of σ_E correspond to particles captured in weak MMRs. For example, particles at the 5:–2:–2 resonance with $e_p = 0.15$ (typical Themis family members) have values of $\sigma_e \sim 0.005$. This means that, in order to diffuse from their present location up to about $e_p \sim 0.3$ (where they would have a good chance to be thrown to the 2:1 resonance), they would spend some 4–6 Byr. In other words, the narrow MMRs alone seem to be rather inefficient to transport asteroids into the 2:1 resonance in time scales of millions of years, except when the asteroids lie close to the border of the 2:1 resonance from the begining. In such cases, the role of the 9:–2:–4 and 13:–7:–5 resonances to inject members of Themis family in the 2:1 resonance could have some relevance which should be studied with more detail (see Fig. 2).

On the other hand, the overlap of narrow MMRs at $e_p > 0.3$ provides a totally different mechanism to transport asteroids. Due to this overlap, the objects there are able to randomly walk in semi-major axis, virtually jumping between the MMRs, and can be eventually pushed to enter the 2:1 resonance in time scales as shorter as some Myr. These short time scales do not allow to plot their trajectories in the proper elements space (recall that proper elements are averages over 10 Myr). Notwithstanding, about 80% of the initial conditions with $e = 0.4$ in Set #1 ended captured at the 2:1 resonance (at least temporarily) in at most a couple of 10 Myr. We wish to stress that this mobility of a_p at large eccentricities is not related to Jupiter crossing orbits. In fact, the 2:1 resonance induce a forced oscillation of e which reaches its maximum when $\varpi = \varpi_{\rm J}$, so this mechanism is in some sense protecting the particles from having a close approach to Jupiter. Actually, Jupiter crossing orbits at $a \sim 3.15$ AU will happen only for maximum values of $e > 0.55$, even taking into account the 0.35 AU Hill's sphere of that planet. The diffusion cannot be attributed to the perturbation of Mars either, since this planet has not been included in the simulations. However, Mars crossing orbits happen for $e > 0.45$, and this planet should be taken into account in future studies of the dynamics at this high eccentricity region.

The overlap of weak MMRs seems to be a quite efficient way to inject large amounts of objects in the 2:1 resonance in very short time scales. The problem is to find a suitable source of asteroids to feed this mechanism. Unfortunately, the density of observed asteroids near the Hecuba gap has a drastic decay for $e > 0.30$ (see for example, Knežević and Milani, 2001), and most of this high-e asteroids are driven to planet crossing trajectories in time scales smaller than 100 Myr. Maybe the weak MMRs in the neighborhood of the Hecuba gap could be able to feed the region of overlap, by exciting the eccentricity of objects with an already high e (~ 0.3). However, even if this is the case, we would need another mechanism to resupply the weak MMRs themselves. In recent years, the role of non conservative forces (like Yarkovsky effect) and mutual scattering, has been raised as a possible solution to feed the large web of weak MMRs in the asteroid belt, through the introduction of a significant semi-major axis mobility of the asteroids. We will return to this subject later in Sect. 2.3.

Before closing this section, we wish to recall that our present study has been restricted to the very neighborhood of the 2:1 resonance, and to the dynamical effect of a few MMRs. We have not analyzed the possible effect of two important two-body MMRs with Jupiter located in the interval

$3.05 < a < 3.12$ AU, namely 11:5 ($a \simeq 3.07$ AU) and 13:6 ($a \simeq 3.11$ AU). Numerical experiments by Michtchenko (in preparation) show that the diffusion at these resonances is much larger than at the 5:–2:–2 resonance, and they could be able to resupply the high-e overlap region with much better efficiency. Last, but not least, these two resonances could be one of the best possible path to transport material form the region of Themis family to the 2:1 resonance.

2.2. Fate of injected particles

We have shown in the last section that weak MMRs at the left side of the Hecuba gap would be able to inject asteroids into the 2:1 resonance. But, which is the typical fate of these particles after they enter the 2:1 resonant space?

The answer to this question can be found by looking again at Figs. 2 and 3. Once the particles were captured by the 2:1 resonance, they followed a fast diffusion path to Jupiter crossing orbits and were discarded from the simulation after one or several close encounters with this planet. The typical lifetime of injected particles (after the injection) is no longer than 10 Myr, and much smaller in most cases. During this short lifetime, the eccentricity is chaoticaly driven to higher values, while in several cases the inclinations become also excited above 10°. This behavior is related to the presence of a highly chaotic region inside the 2:1 resonance, which is generated by the overlap of several secular and secondary resonances. For $e > 0.20$, the resonant dynamics near the separatrix is dominated by the overlap of secular resonances, mainly ν_5, ν_6 and Kozai resonances (Morbidelli and Moons, 1993). For $0.05 < e < 0.20$, is the overlap of secondary resonances which dominates. A secondary resonance occurs when the period of libration of σ is an integer multiple of the period of circulation of ϖ. Each of these resonances alone does not have a significant effect in the diffusion, but in the case of the 2:1 resonance, the overlap of several $p/1$ secondary resonances ($p \geq 2$) generates an important region of chaos at low eccentricities (Michtchenko and Ferraz-Mello, 1996). This region behaves as a barrier, separating the low eccentricity region from the central region of the 2:1 resonance, where the Zhongguos are found (Ferraz-Mello, 1994). The effect of this barrier is to excite the inclination of the particles there up to values $\sim 30°$ or larger. This excitation is known to happen in relatively short time-scales, and allows to transport particles from the region at $e < 0.1$ to the region at $e > 0.4$ of the 2:1 resonance through a "bridge" at high-inclinations (Henrard et al., 1995).

The actual effect of the barrier of chaos related to the secular and secondary resonances is illustrated in Fig. 5. We show there the evolution in the space of proper a, I of some initial conditions in Sets #1 and #2. The top panel corresponds to the initial conditions at $e = 0.25$, and the bottom one, to those with initial $e = 0.20$. Proper elements were defined here as minimum a and maximum I over 10 Myr. For $e = 0.25$, we clearly distinguish two regions where the particles evolve without exciting their inclinations. One is outside the 2:1 resonance, between 3.15 and 3.18 AU approximately. The other is inside the 2:1 resonance, between 3.21 and 3.23 AU. This last region corresponds more or less to the one where the Zhongguos are located. Both regions are separated

by a "gap" of about 0.03 AU in width, where the inclinations are highly excited. This last region is related to the overlap of secular resonances near the separatrix of the 2:1 resonance, located ~ 3.18 AU. A smaller excitation of the inclinations is also observed for values $a \sim 3.25$ AU, in this case related to the secular resonance ν_{16}. For $e = 0.20$ the situation is slightly different. Still we can see a region outside the resonance, between 3.15 and 3.20 AU, where the proper inclinations remain small. But inside the 2:1 resonance, we observe a region of some 0.05 AU in width where the excitation of inclinations is rather huge. This region is related to the overlap of secondary resonances. Since the density of points in the space of proper elements is a rough indicator of the diffusion speed, we can conclude, by comparing both panels, that the excitation in the region of the separatrix is faster than that in the region of the secondary resonances. We will try in the following to better quantify this diffusion speed.

Following the same recipe applied in RNF-I, we proceeded to mount a map of the residence time in the space of proper elements. In short, we took the space of proper a, e in the range $3.14 \leq a_p \leq 3.28$ AU and $0.025 \leq e_p \leq 0.425$, and we divided it in 28×8 equal cells, each one with $\Delta a = 0.005$ AU and $\Delta e = 0.05$. Then, we use the time series of proper elements of all the particles in Sets #1 and #2 to determine the time that each particle spent in each cell. The time of residence was computed over the 200 Myr interval spanned by our simulation or *until the proper inclination of the particle became larger than* 10°. Since two or more particles can provide different values of residence time for the same cell, in the end we consider their averages. This map of residence times is shown in Fig. 6. The cyan-blue colors correspond to the largest residence times, while the reddish colors correspond to the shortest ones. The blank cells were never occupied by any particle in the simulation. We also show in this plot the approximate locations of the center and separatrix of the 2:1 resonance (calculated analytically), the separatrices of the ν_{16} resonance, the secondary resonances 2/1,...,5/1, and the instability border (IB) which delimits the region of overlap of secular resonances (these latter estimated numerically). To mount this map we have used two sets of proper elements. The first one was defined as the minimum of a and the maxima of e, I over 10 Myr, with a 0.1 Myr sampling. Unfortunately, this set is not able to resolve the residence time in the cells corresponding to region of overlap of secular and secondary resonances. This is because the average residence times there are shorter than 10 Myr. Then, we used a second set of proper elements, defined as the minima/maxima over 1 Myr (also with a 0.1 Myr sampling), to "complete" the cells where the former one failed to provide a residence time.

Several interesting features can be observed in Fig. 6. Outside the 2:1 resonance it is possible to identify a pattern of inclined stripes related to the 5:–2:–2 and 7:–2:–3 resonances. We can also see regions of rather strong stability (darker cells) surrounding these MMRs at low eccentricities. Inside the 2:1 resonance, we observe a region of long residence times between the ν_{16} and the IB line. This is the region where the Zhongguos and Griquas are located (white and black dots, respectively). The residence times there are larger than above the ν_{16} line, in agreement with the results obtained in RNF-I from a different simulation. But the most remarkable feature in Fig. 6 is the wide stripe of short residence times that separates the stable regions outside and inside the 2:1 resonance. The

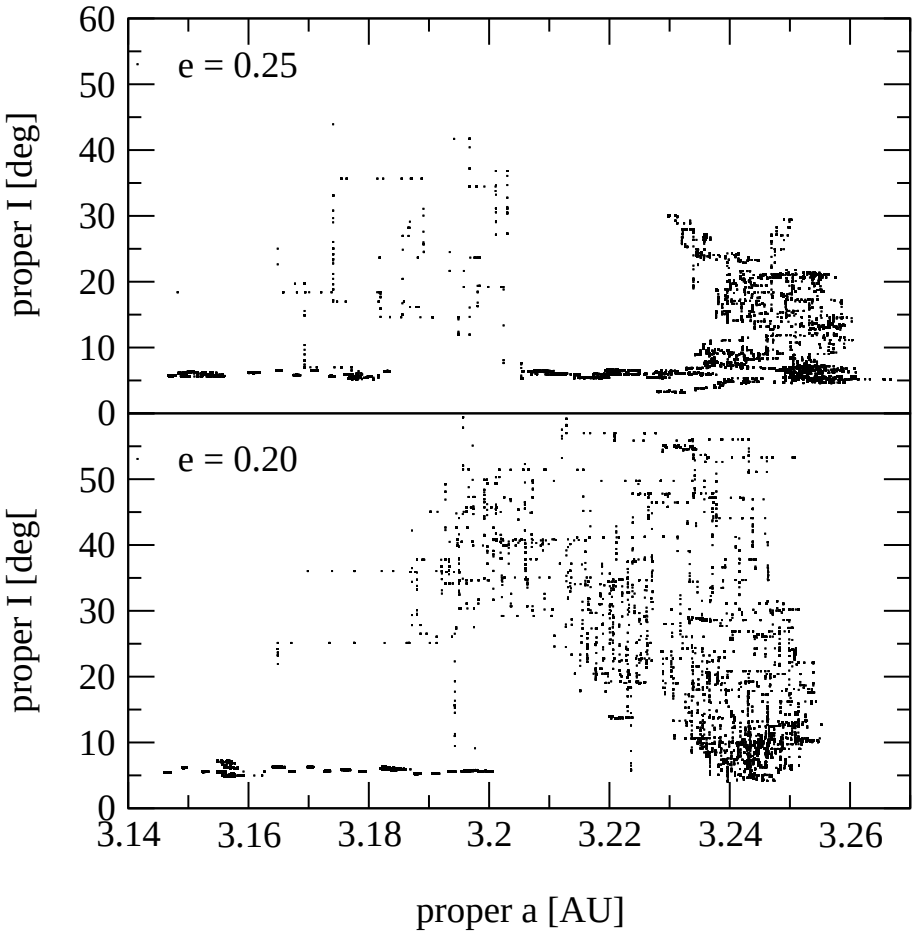

Fig. 5.— Evolution of test particles in the space of proper a, I. The particles correspond to 70 initial conditions in Sets #1 and #2 for two different levels of initial eccentricity (35 particles in each level). Proper elements are defined as maximum of I and minimum of a over 10 Myr, and are sampled every 0.1 Myr. In the top panel, the proper inclinations are excited in the region of overlap of secular resonances, and also at the ν_{16} resonance. In the bottom panel, the excitation correspond to the overlap of secondary resonances.

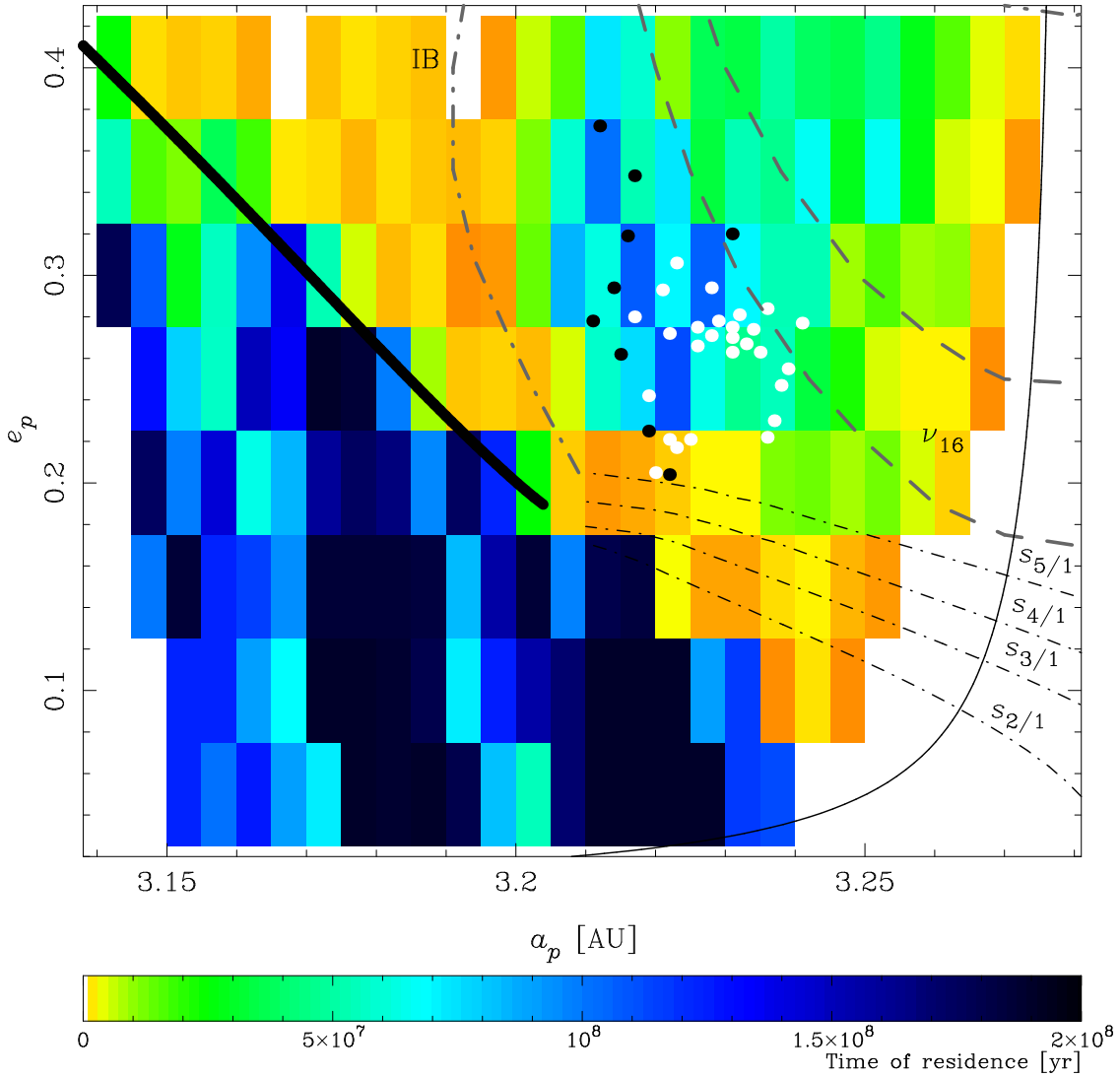

Fig. 6.— Map of residence times, computed from the proper elements in a 200 Myr simulation of test particles outside and inside the 2:1 resonance. We used two sets of proper elements, defined as minimum of a and maxima of e, I over 10 Myr and 1 Myr, respectively. Both sets had a 0.1 Myr sampling. The plot also shows the location of the equilibrium centers of the 2:1 resonance (full thin line), the separatrix (full bold line), the separatrices of the ν_{16} secular resonance (dashed lines), the instability border (IB), and four secondary resonances (dotted-dashed lines marked $s_{k/1}$). The white and black dots represent the real Zhongguos and Griquas, respectively.

typical residence times in this stripe are of the order of 1 Myr or even smaller. It is worth recalling that the residence times in Fig. 6 were computed while $I_p \leq 10°$. Then, they are also likely to represent the time necessary to excite the proper inclinations beyond 10°.

The above results put strong constrains to the possible origin of the resonant population in the Hecuba gap. On one hand, it is clear that the mechanisms of injection analyzed in Sect. 2.1 can help to resupply the population of unstable asteroids in the 2:1 resonance. Their rather high inclinations and short lifetimes are in good agreement with the expected behavior of particles injected into the 2:1 resonance, either by crossing the separatrix or the region of secondary resonances. It is worth noting that inclinations will always be highly excited for particles in the region of secondary resonances. However, inclinations not always become excited when the particles are injected in the region of secular resonances. This is because in that region the diffusion in e_p is much faster than in I_p, then particles can be fastly driven to Jupiter crossing orbits without having enough time to get their inclinations excited. A typical case is shown in Fig. 7, and such mechanism could explain why we presently observe several resonant asteroids having rather low inclinations but very short lifetimes (as the case of (5201) Ferraz-Mello, see Table 1 of RNF-I).

On the other hand, the origin of the Zhongguos cannot be supported under a scenario of "smooth" injection. If we assume that these objects arrived to their present location from outside the 2:1 resonance (for example from Themis family), they had to be able to cross a region of about 0.03 AU in a or 0.05 in e in a time-scale not larger than a couple of Myr (in the most optimistic case), in order to retain their presently observed low inclinations ($I_p \leq 5°$). This is the most important dynamical constrain to the origin of the Zhongguos (the other important constrain is observational, and refers to their size distribution, see RNF-I). The remaining of this paper will be dedicated to analyze some possible mechanisms that could account for the necessary drift to inject the Zhongguos in their present location.

2.3. Yarkovsky orbital drift and mutual scattering

As we already mentioned in Sect. 2.1, non conservative forces and perturbations other than purely planetary ones, could play a non negligible role in the origin of resonant asteroids at the Hecuba gap. Non conservative forces, for example, allow the mobility of the semi-major axes and help to interchange material between regions of regular and chaotic motion. In this section we will discuss the possible role of two mechanisms that favor the mobility of a: (i) Yarkovsky effect and (ii) mutual scattering.

Yarkovsky effect (hereinafter YE) arises from the thermal recoil of a rotating body, which receives the solar radiation from a given direction and re-emits part of it to a different one. There are two variants of the effect: the diurnal, related to the rotation period, and the seasonal, related to the orbital period. The former behaves as a dissipative or anti-dissipative force, depending on the sense of rotation (retrograde or prograde), while the latter is always dissipative (Rubincam, 1995).

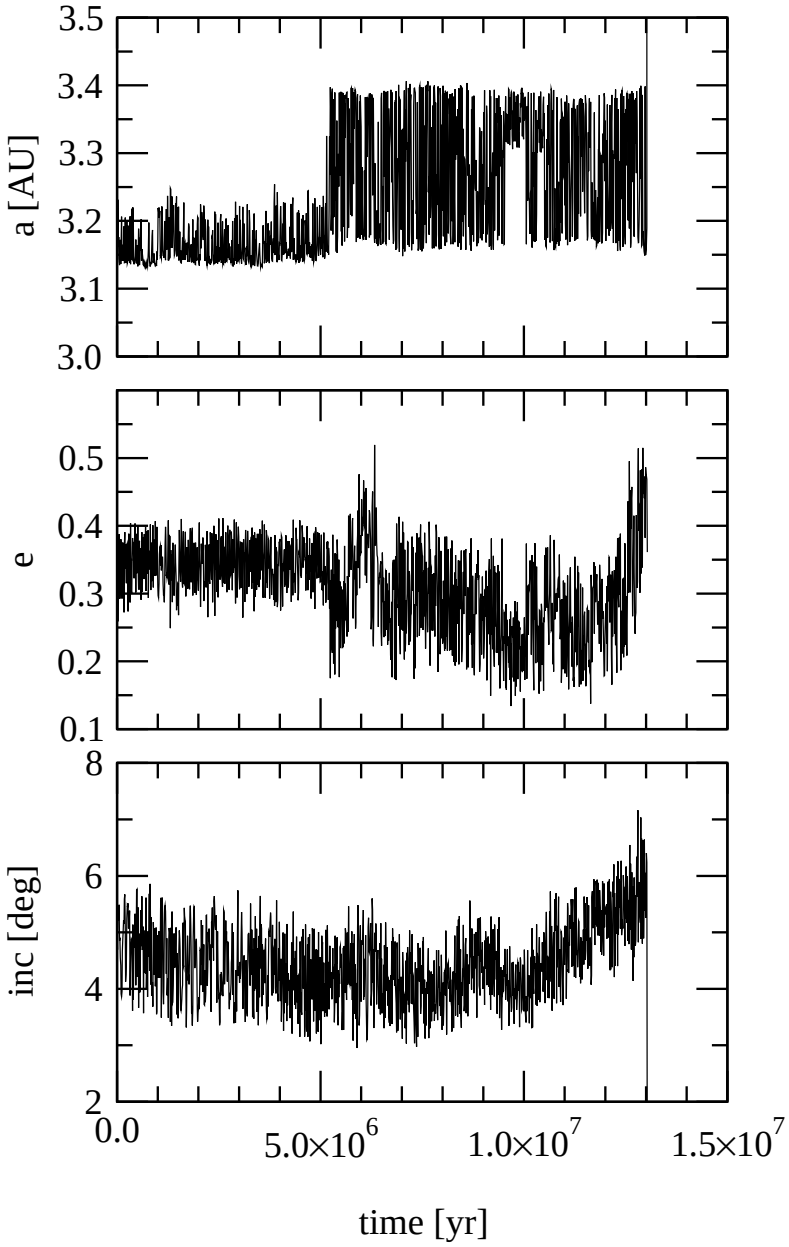

Fig. 7.— Evolution of the osculating elements for a short-lived test particle injected in the 2:1 resonance. The particle was initially at $e = 0.4$. Note that e is largely excited, but the excitation of I is much slower, and the particle escaped while still having a low inclination.

Both effects cause a net drift in proper a which is inversely proportional to the size of the body. In Sect. 3.2 of RNF-I, we have already described simulations with Yarkovsky effect, so we refer the reader to that paper for more details.

To analyze the actual importance of this effect in enhancing the diffusion at the left side of the Hecuba gap, and in favoring the injection of asteroids into the 2:1 resonance, we performed the following simulation. We took 50 initial conditions from Set #1 in the range $0.15 \leq e \leq 0.30$, and integrated them again, this time adding YE to the simulation. We used a version of the Swift integrator that we adapted for this purpose. The YE accelerations were modeled according to Vokrouhlický et al. (2000). The parameters of the model were typical of regolith-covered bodies, with a very low surface conductivity, in order to have a dominant diurnal effect (refer to RNF-I for the precise values of these parameters). We assumed a diameter of 6 km for all the particles, and randomly-oriented prograde spin axes to obtain a net anti-dissipative force. The simulation spanned 100 Myr with a time step of 0.05 yr. We computed proper elements as usual (averages over 10 Myr, with 0.1 Myr sampling), and estimated the diffusion parameters $\sigma_a, \sigma_e, \sigma_I$ and $\beta_a, \beta_e, \beta_I$ as explained in Sect. 2.1 (see also RNF-I). In this case, the parameter β_a has a quite special meaning, because it gives the effective average drift rate induced by YE.

Figure 8 presents the results of this simulation. The abscissas of each plot are the diffusion parameters for each particle in the simulation without YE, while the ordinates are the same parameters in the simulation with YE. In all panels we can appreciate a tendency to larger values of the parameters in the simulation with YE. This is remarkable in the case of proper a, as expected, but is also observed in the case of e_p and (although less evident) in the case of I_p also. We recall that YE by itself should not cause any significant drift of the eccentricities and inclinations. The larger values of diffusion in e_p, I_p observed in the middle and bottom panels of Fig. 8 are rather due to the interaction between YE and the weak MMRs. More precisely, an object near a MMR can be pushed by YE until it reaches the MMR; then it can be driven to enter it or to jump over it. In any case, this causes and excitation of their otherwise stable e_p and I_p. It is worth noting that the inverse process, that is, to extract a body from a MMR with YE, is not so straightforward. In fact, once an object becomes capture in a MMR, it is rather difficult that YE can draw it out. This can be better understood if we recall that non conservative systems tends to configurations of minimum energy, and the MMRs themselves are basins of energy. The interaction between YE and weak MMRs is still not well understood. Unfortunately, the construction of analytical models is quite complex in this case, and the classical models for low order MMRs (see Gomes, 1995, 1997a, and references therein) are not directly applicable.

On the other hand, these classical models are helpful to understand the interaction between YE and the 2:1 resonance, at least in a first approach. We recall that inside the 2:1 resonance, the "natural" effect of any anti-dissipative force will be to excite the eccentricities while keeping constant the amplitude of libration. In other words, consider an ideal 2:1 resonance, with no secular or secondary resonances inside it, and consider a particle approaching to its left border pushed by YE. Then, once the particle enter the resonance, its eccentricity will be excited to higher values and

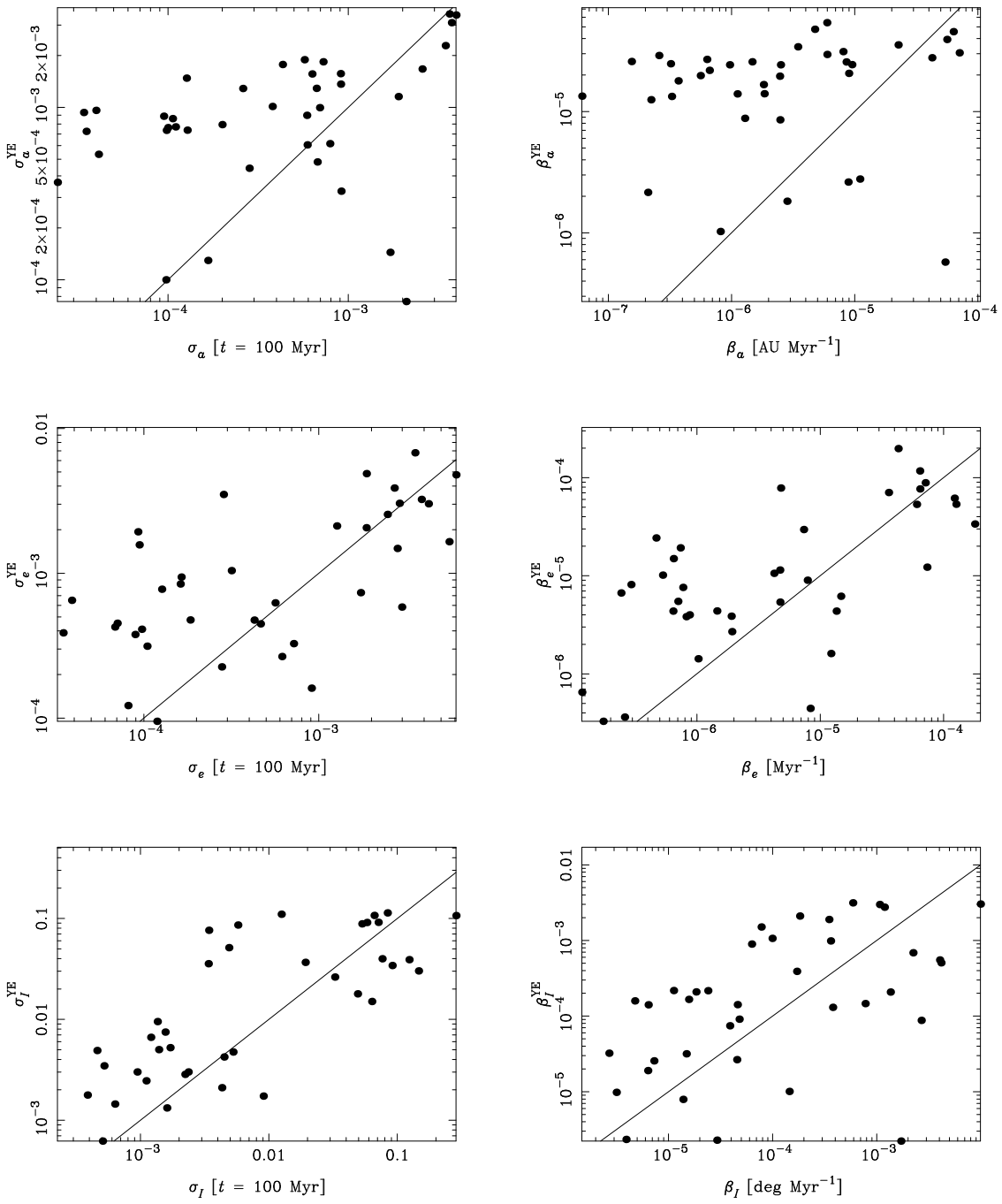

Fig. 8.— Diffusion parameters σ_E and β_E for each proper element E in the simulation without YE (in the abscissas), and comparison with the same quantities in the simulation with YE (in the ordinates). Each dot corresponds to one particle in the simulations. Only particles that survived over 100 Myr in both simulations are shown. The full lines correspond to the identity function.

its amplitude of libration will behave as an adiabatic invariant. This mechanism can make a nearby non resonant asteroid at $e \sim 0.15$ (e.g. a Themis family member), to become a Zhongguo-like asteroid with $e \sim 0.25$. But in the real 2:1 resonance, this implies to cross the region of secondary resonances, where the asteroid will not avoid to excite its inclination, unless it cross sufficiently fast. How fast? The rate of change in a_p which is necessary to achieve a given change in e_p can be easily estimated from Lagrange equations in the averaged circular planar restricted 3-body problem near the 2:1 resonance (see Greenberg and Franklin, 1976). It is given by:

$$\left\langle \frac{da}{dt} \right\rangle = 2 \langle a \rangle \langle e \rangle \left\langle \frac{de}{dt} \right\rangle , \tag{2}$$

where $\langle \ldots \rangle$ stands for the average, and we can consider $\langle a \rangle \equiv a_p$ and $\langle e \rangle \equiv e_p$. Now, according to the results of Sect. 2.2, the particle would need a drift $de_p/dt \sim 0.02$ Myr^{-1} in order to cross the region of secondary resonances without having its inclination excited, which implies $da_p/dt \sim 0.02$ AU Myr^{-1}. From Fig. 8 (top-right panel), it is easy to estimate that the average rate of drift in a_p provided by YE for 6 km bodies at the left side of the Hecuba gap is between $8 \times 10^{-6} \leq \beta_a \leq 5 \times 10^{-5}$ AU Myr^{-1}. This represents about 0.02 AU per Byr, in good agreement with the estimates of Farinella and Vokrouhlický (1999) for regolith bodies. Such rate is enough to keep objects moving around in a_p during the age of the Solar System. But on the other hand, it is too slow to allow a particle to safely cross the region of secondary and/or secular resonances inside the 2:1 resonance, without highly exciting its e_p and I_p. In other words, to inject the observed Zhongguos in their present location, we would require to move objects larger than 6 km at a rate of about 2/100 AU per Myr, which is four orders of magnitude larger than that provided by YE.

In order to confirm these estimates, we took some particles from our simulation, starting very close to the 2:1 resonance border, and extended their integration up to 300 Myr. In Fig. 9, we show the evolution of a_p (averages over 1 Myr, with 0.1 Myr sampling) for three different values of proper eccentricity. After 100 Myr several particles became injected in the 2:1 resonance, but their lifetimes after the injection is not larger than some 10 Myr. In all cases, the injected particles had their proper inclinations excited to values larger than 20° in a few Myr, as expected. Our conclusion is that it would be highly improbable that YE helps to inject the Zhongguos in the 2:1 resonance. However, we want to stress that our simulations were limited, both by the small number of test particles and by the chosen values for the YE parameters, and we believe that more detailed studies would be necessary to draw any definitive conclusion.

The case of mutual scattering is not so different from YE. Mutual scattering arise from the gravitational perturbation of small asteroids between them or by the largest asteroids in the main belt. Recently, it has been proposed by Carruba et al. (2000) that mutual scattering could contribute to the semi-major axis mobility of main belt asteroids. Preliminary studies by these authors show that only the largest asteroids (Ceres, Pallas and Vesta) seem to have a dominant scattering effect throughout the main belt, although this effect would not be large. According to Monte Carlo simulations (Bottke, personal communication), the average dispersion in proper a induced in a typical Themis family member by close encounters with Ceres should be about 1/100 AU per Byr

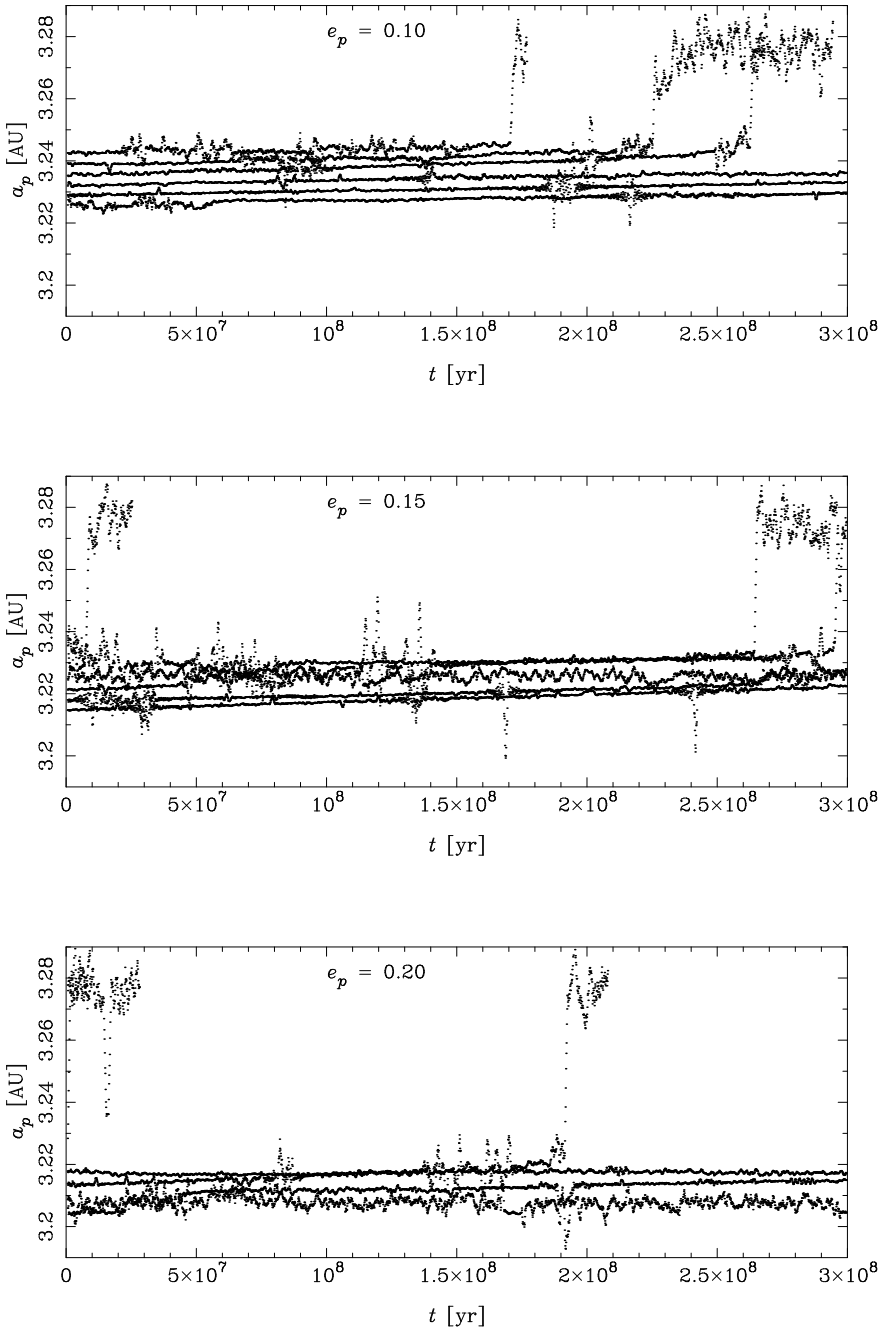

Fig. 9.— The evolution of proper a (averages over 1 Myr) for test particles near the border of the 2:1 resonance under the effect of Yarkovsky forces. All particles have 6 km in diameter and prograde rotation. Their proper eccentricities are indicated in each panel. Some particles are effectively injected in the 2:1 resonance, but they do not survive there for more than some 10 Myr. All the particles injected had their inclinations excited up to 20° or more.

(or maybe less, since Monte Carlo codes tend to overestimate these quantities). This rate of diffusion is even smaller than that of YE, and according to the above considerations we can conclude that mutual scattering is mostly irrelevant to the process of injection of resonant asteroids in the Hecuba gap.

3. Resonant capture due to planetary migration

We will discuss in this section another mechanism to "inject" asteroids in the 2:1 resonance, that is, the capture due to migration of the resonance. It is widely accepted now that the major planets did migrate (changed their semi-major axes) during a certain period of their history (Fernández and Ip, 1984, 1996). This migration arose from the exchange of energy and momentum between the Jovian planets and the swarm of planetesimals that remained in the region beyond 10 AU immediately after the formation of these planets. The planetesimals were scattered by close encounters with all four major planets, but the scattering by Jupiter was much more efficient than that of Saturn, Uranus and Neptune. This caused a net loss of planetesimals, which were presumably ejected to the Oort cloud, and the corresponding energy balance was transferred to the drift in the planetary semi-major axes. Under this scenario, Jupiter migrated inwards, from about 5.4 AU to its present 5.2 AU, while the other planets migrated outwards by some 0.8 AU (Saturn), 3.0 AU (Uranus) and 7.0 AU (Neptune) up to their present positions. It is still under discussion when did this migration take place, but in any case, it should be dated more than 3.8 Byr ago (Levison et al., 2001), and it should have had important consequences in the dynamics of the whole Solar System. One of these consequences was the migration of the MMRs. As the semi-major axis of the planet drifted, it pulled the MMRs and these latter swept the regions where they passed by. When a sweeping MMR reaches an object, it can be either captured in the resonance, or it can jump over the resonance, depending on the type of resonance (inner or outer), the order of the resonance, and the sense of the sweeping.

If we assume the above estimates to be correct, then the 2:1 resonance should have been migrated inwards from 3.40 AU to 3.28 AU, sweeping a region larger than half its width. During this process, we should expect that several asteroids with low eccentricity became captured in the resonance. In fact, the migration of the 2:1 resonance inwards behaves almost in the same way as the application of an anti-dissipative force on the asteroids. For $e < 0.2$ the 2:1 resonance is "open" on the left side (there is no separatrix), and during the sweeping inwards it would pick up asteroids virtually like a "shovel". According to the theory, the captured asteroids would evolve exciting their eccentricities monotonically, while their amplitudes of libration are kept almost constant (adiabatic invariant). The relation between the values of the asteroid's orbital elements before and after the capture, is given approximately by the conservation of the canonical momentum N (Eq. 1). This relation can be used to estimate the final eccentricities of the captured population as a function of the total shift of the resonance in a.

The sweeping of MMRs is believed to have been responsible for the resonant capture of some

groups of minor bodies, like the group of Hilda at the 3:2 resonance with Jupiter (Liou and Malhotra, 1997), and Plutinos at the 2:3 resonance with Neptune (Malhotra, 1995; Gomes, 2000). In the case of the 2:1 resonance, we can guess that a large population of asteroids was indeed captured during the planetary migration, but it was not able to survive until our days due to the global stochasticity of the resonant phase space (Ferraz-Mello et al, 1998b). The question is: could the Zhongguos be the lucky survivors of such presumably captured population of asteroids?

According to their typical dynamical lifetimes (see RNF-I), they could. Unfortunately, this is not enough evidence to conclude that they are. In fact, the resonant capture due to planetary migration is a mechanism much more complex than the simplified view given above. It involves several dynamical processes, like sweeping of secular resonances and planetary inequalities, that would have helped to strongly destabilize the asteroids' orbits. For example, outside the 2:1 resonance, the sweeping of the secular resonance ν_6 was responsible for a huge excitation of the asteroids' e, I throughout the main belt (Gomes, 1997b). Inside the Hecuba gap, slight changes in the value of the Great Inequality (5:2 commensurability) between Jupiter and Saturn were able to largely increase the chaotic diffusion (Ferraz-Mello et al., 1998a). Also, in order to become captured at $e \sim 0.3$, the asteroids needed to pass through the region of secondary resonances at $e \sim 0.15$, with the consequent constrain to their lifetimes (Sect. 2.2). Moreover, we should expect that a non negligible amount of the planetesimals scattered during the migration were thrown towards the inner Solar System (Levison et al., 2001), and contributed to largely perturb the asteroids and to increase the collisions throughout the main belt. In other words, if the origin of the Zhongguos is related to the planetary migration, then they probably needed to pass by several hard tests before being able to remain trapped in a quite small region of the phase space where they could evolve in peace until our days.

To better discuss the viability for capturing the Zhongguos through migration of the resonance, we simulated the evolution of a swarm of 200 test particles under the effect of planetary migration. For each particle, the initial semi-major axis was chosen at random in the interval $3.15 \leq a \leq 3.46$ AU, which was more or less the interval swept by this resonance if Jupiter migrated by 0.2 AU. The initial e, I were also chosen at random, dividing the swarm into two populations of 100 initial conditions each: (i) a "cold" population in the intervals $0 \leq e \leq 0.1$ and $0 \leq I \leq 2.5^\circ$, and a "hot" population, with $0.1 < e \leq 0.2$ and $2.5^\circ < I \leq 5^\circ$. In both cases the remaining initial angles were also chosen at random between $0, 360^\circ$. The total migration time was set to 20 Myr, but the simulation was continued for 2 Myr more after the migration ceased. The migration was included in the model by adding to the planets' accelerations an artificial non conservative term, $\overrightarrow{A}_{\rm nc}$, given by:

$$\overrightarrow{A}_{\rm nc} = \sqrt{GM} C_{\rm nc}\, e^{-(t-t_0)/\tau}\, \frac{\overrightarrow{V}}{|V|} \qquad (3)$$

where G is the gravitational constant, M the solar mass, $\overrightarrow{V}$ the velocity of the planet, t the time, t_0 refers to the time at the beginning of the migration (for our purposes will be $t_0 = 0$), τ is the

characteristic time-scale of the migration (do not confuse with the total migration time), and

$$C_{\rm nc} = \frac{1}{\tau}\left(\frac{1}{\sqrt{a_i}} - \frac{1}{\sqrt{a_f}}\right) \tag{4}$$

is a constant that depends on the initial and final values of the planet's semi-major axis, a_i, a_f (see Malhotra, 1995). We used a modified version of the Swift integrator that we adapted for this purpose[3].

Equation (3) provides an exponential variation of a that converges asymptotically to a_f. For our simulation, we choose a_f equal to the present mean semi-major axes (Bretagnon, 1982), and $a_i = 5.4$ AU for Jupiter, 8.7 for Saturn, 16.3 for Uranus, and 23.2 for Neptune. These values made Jupiter and Saturn migrate in such a way that they started near the mutual 2:1 commensurability and ended near the mutual 5:2 commensurability, but without entering or crossing them (however, they did cross the 7:3 and 9:4 commensurabilities). The characteristic time-scale τ is a critical parameter, because it determines the actual speed of the migration: 63% of the migration happens in that time-scale. In our case it was set to $\tau = 2$ Myr, according to typical values found in the literature. However, recent studies indicate that this time-scale could be up to 10 times larger (Hahn and Malhotra, 1999). Another critical problem concerns the setup of the initial position and velocity of the planets. In our case, we applied a strategy already used by several authors, consisting in integrate the four major planets backwards, starting in their present positions and applying the non conservative forces in the opposite sense[4]. The "final" conditions so obtained could be used as "initial" conditions of the migration, but unfortunately the integrations are not reversible. This is easy to understand if we think that the planets cross several mutual resonances along its migration paths. While in the backwards integration the planets could be able to jump over such mutual resonances, in the forward integration they could be able to be captured in some mutual resonance (and vice-versa). The probability of capture is somehow related to characteristic time-scale τ: the longer the latter, the larger the former. Then, after obtaining our "initial" conditions with the backward integration, we had to perform a series of forward simulations, making a fine tuning of the constants $C_{\rm nc}$ until we arrived to a configuration where the values of the planetary mean semi-major axes were compatible with the present ones.

The results of our simulation with test particles and migrating planets are summarized in Fig. 10. We indicate there the position of the particles in the space of proper elements a_p, e_p and a_p, I_p, for three different times along the simulation. The proper elements were defined as the minimum of a and the maxima of e, I over 1 Myr, with 0.1 Myr sampling. We also indicate the approximate location of the resonance and the separatrices in the a, e plane.

---

[3]Note that this acceleration depends on the velocity, so the leap-frog propagation scheme used by Swift is no longer symplectic. Although this approach has been widely used by many authors, its main disadvantage is that the algorithm slows its efficiency because the accelerations need to be computed twice per time step.

[4]In practice this was accomplished just by setting $t_0 = -20$ Myr and integrating from $t = 0$ to $t = -20$ Myr.

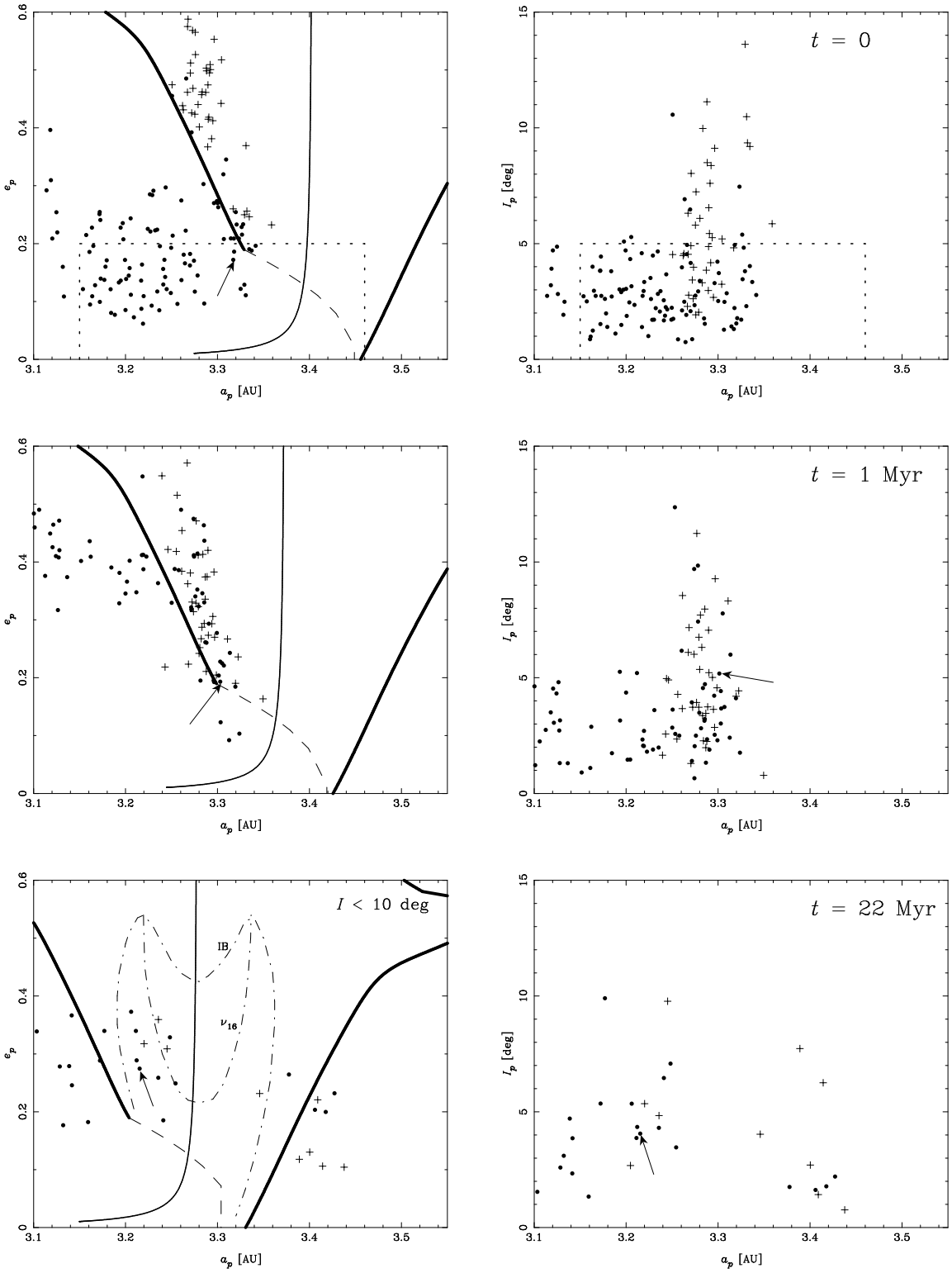

Fig. 10.—

Fig. 10.— Three stages in the simulation of test particles including planetary migration. Top panels: proper elements at the beginning of the simulation; middle panels: status after 1 Myr of migration; bottom panels: final proper elements, 2 Myr after the migration ceased. Proper elements are defined as minimum of a and maxima of e, I over 1 Myr, with 0.1 Myr sampling. Crosses are particles that started the simulation inside the 2:1 resonance, and dots are particles that started outside. The dotted rectangle in the top panels indicates the approximate distribution of the osculating initial conditions of the simulation. In the leftmost panels we indicate the approximate location of the center (full thin line) and the separatrices of the resonance (bold lines). The dashed line indicates the approximate limit between the region of libration and alternation/circulation of σ. In the bottom-left panel, we also plot the location of the ν_{16} resonance and the instability border (IB). Only particles with $I_p < 10^\circ$ are shown in the bottom panels. Finally, the arrow indicates the particle shown in Fig. 11

.

The first two panels show the state of the system at the beginning of the simulation ($t = 0$). Crosses represent particles that are already inside the 2:1 resonance (97 particles), while dots are particles that started the simulation outside the resonance (103 particles). To identify the resonant particles, we integrated the initial conditions of planets and particles over 1 Myr without including migration, and looked at the behavior of the angle σ. This simulation also provided the initial set of proper elements at $t = 0$.

The remaining panels in Fig. 10 show the state of the system after 1 Myr of migration and at the end of the simulation (22 Myr; recall that we ceased the migration at 20 Myr). The last two panels only show those particles that ended with a proper inclination smaller than 10°. Several features can be appreciated in these plots. At $t = 1$ Myr, the particles located at the left side of the resonance have suffered a large excitation of their proper eccentricities (their average e is between 0.2-0.3). This kind of behavior has been already identified by Gomes (1997b) and Levison et al (2001), and was attributed to the sweeping of secular resonances. In our simulation only the eccentricities were excited, while the inclinations remained small. This is most probably related to the sweeping of some strong secular resonance of the perihelion, maybe ν_6. We can also see that, at $t = 1$ Myr, a large part of this e-excited population is entering the 2:1 resonance, jumping through the separatrix. Most of these captured particles remained near the separatrix and did not survive too much inside the resonance, being fastly driven to Jupiter crossing orbits. On the other hand, some particles at the left side of the resonance did not have their eccentricities excited, and became to approach the resonance at $e_p < 0.2$. This is the case of the particle indicate by an arrow in Fig. 10. At $t = 22$ Myr this particle has already entered the resonance and remained in the region of the Zhongguos, with a final proper I less than 5°. The actual behavior of this "baby Zhongguo" during the migration is shown in Fig. 11. We can appreciate there the exact moment when it entered the resonance, between $t = 0.7$ and 1 Myr. After entering the resonance, it took less than 5 Myr to arrive to its final location. Since it ended in the most stable region of the 2:1 resonance, we can

expect that this particle will be able to survive there over the age of the Solar System.

Back to Fig. 10, some other particles were also captured in the resonance at the end of the simulation, keeping their low initial inclinations. From the initial 103 particles starting the simulation outside the resonance (dots), 16% ended captured at $t = 22$, and only 8% did it with $I_p < 10°$. However, the proportion of "cold" and "hot" particles in these statistics is different: 16% of the cold population was captured against 14% of the hot population. But 9% of the hot particles ended captured with $I_p < 10°$, against 6% of the cold ones. This difference could be related to the eventual interaction with secondary resonances during the capture process. From the preservation of the invariant N (Eq. 1), it is easy to show that cold particles take more time to excite their eccentricities during the capture, having more time to interact with the web of secondary resonances. It is true that the secondary resonances themselves will move during the migration, but their net shift should not be large. In fact, the 2:1 resonance itself dictates the proper rate of motion of the asteroids' perihelia inside it, and this rate is less changed by the migration.

Concerning the 97 particles starting the simulation inside the resonance (crosses), only a few amount (4%) were still there after 22 Myr. Some of them also survived at the right side of the resonance, like having been left by the resonance during its migration leftwards.

Our results concerning the capture of Zhongguo-type objects due to migration provide the first evidence of a mechanism able to inject such objects inside the 2:1 resonance. However, as we already mentioned, resonant capture due to migration involves many different dynamical processes that interact between them in a complex way. Our simulation considered a quite small number of test particles, which does not allow to make a good statistical analysis of the results. Moreover, we only tested a very particular model of migration (exponential) with a very particular value of the characteristic time-scale. Would we obtain similar results, for example, if we use a value of τ ten times larger? The answer to this and to other similar questions is beyond the scope of this work, and the problem is still open for future, more detailed, studies. In the next section we will discuss another mechanism to inject objects inside a resonance, related to the breakup of asteroids in the neighborhood of the resonance.

4. Catastrophic injection

It has been proposed (Morbidelli et al., 1995; Moons et al., 1998) that the Zhongguos could be the resonant counterpart of the Themis family. That is, the breakup of Themis near the 2:1 resonance would have probably injected a lot of asteroids inside the resonance, and the Zhongguos would be the remnants of this injected swarm. The basic arguments to support this hypothesis are three: (i) The proper eccentricity of (3789) Zhongguo is very similar to the typical proper eccentricity of the Themis family members, that is $e_p \sim 0.2$. In this case, e_p is understood as the maximum of e. (ii) The distribution of Themis family in proper semi-major axis (i.e., minimum of a) has a cutoff at the separatrix of the 2:1 resonance, but (3789) Zhongguo seem to be at the

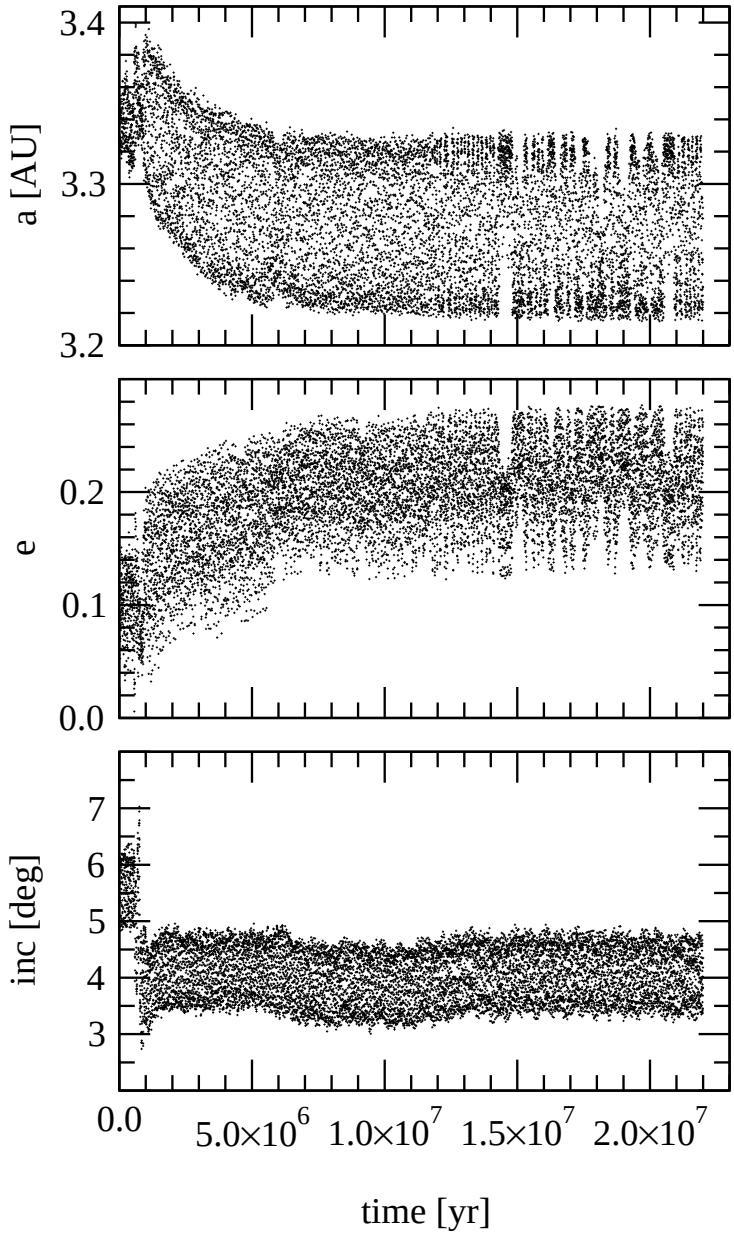

Fig. 11.— The evolution of osculating elements for the particle indicated by an arrow in Fig. 10. The particle ended captured in the region of Zhongguos.

tail of the "natural" prolongation of the distribution inside the resonance. (iii) The Zhongguos are very small objects (less than 15 km) and their collisional lifetimes should be smaller than the age of the Solar System ($\sim 1 - -2$ Byr). Then, it is difficult to assume that they have actually been in the resonance for the last 4.5 Byr. Arguments (i) and (ii) are not very strong indeed, because they require that the breakup occurred at a very particular configuration, when the parent body was at its maximum excursion in eccentricity. Moreover, they are based on the present observed distribution of Themis family members, and they do not take into account that the original distribution (after the breakup) could have been much more compact. In fact, the present distribution can be the result of the dynamical diffusion at the left side of the Hecuba gap (weak MMRs, Yarkovsky, etc.), similar to the case of the Flora family in the inner belt (Nesvorný et al, 2001). On the other hand, argument (iii) is one of the strongest arguments in favor of the catastrophic injection of the Zhongguos. We have already discussed this problem in RNF-I, so we refer the reader to that paper for more details.

In this section, we are going to present some simple simulations aiming to determine under which conditions a breakup of a Themis-like parent body can eject fragments with the necessary velocity to reach the region of Zhongguos inside the 2:1 resonance. For this purpose, we are going to use a very simple model of breakup with isotropic ejection of fragments, as we explain in the following.

The kinetic energy of the fragments after the breakup event can be written as

$$\sum_i \frac{1}{2} m_i v_i^2 = M Q_{\rm D}^* f_{\rm KE} \tag{5}$$

(see Petit and Farinella, 1993) where m_i and v_i are the masses and velocities of the fragments, $M = \sum_i m_i$ is the mass of the parent body, $Q_{\rm D}^*$ is the specific energy of the impact, and $f_{\rm KE}$ is the so-called parameter of *anelasticity*, and represents the fraction of the kinetic energy of the projectile that is transferred to the kinetic energy of the fragments. For a parent body of radius $R_{\rm PB}$ and density $\rho_{\rm PB}$ the specific energy can be estimated as:

$$Q_{\rm D}^* = B\, \rho_p \left(\frac{R_p}{1{\rm cm}} \right)^b \tag{6}$$

where B, b are parameters that depend on the chemical properties of the parent body. According to Benz and Asphaug (1999; see also Love and Ahrens, 1996) typical values for stony bodies are $B = 0.3 - 0.5$ erg cm^3 g^{-2}(we will use 0.4) and $b = 1.36$. The parameter $f_{\rm KE}$ is the most critical one, because it determines the actual dispersion of the fragments after the breakup: the smaller the $f_{\rm KE}$ the more compact the family formed. Unfortunately, this parameter is poorly known. Recent studies using hydrocode models estimate values of $f_{\rm KE}$ between 0.065 to 0.10 for S-type bodies (P. Michel, personal communication), and smaller values (~ 0.01) should be expected for C-type objects (like Themis) since, according to laboratory experiments, they should absorb much more energy.

The first assumption in our model is that the distribution of ejection velocities $N(v_{ej})$ can be

modeled by a Maxwellian, with mean velocity $\overline{v}_{ej}$. given by:

$$\overline{v}_{ej}^2 = \frac{\sum_i m_i v_i^2}{\sum_i m_i} \tag{7}$$

We further assume that the ejection velocity is independent of the mass of the fragments. Although this assumption is consistent with the results of Giblin et al. (1998), there exist evidence of a possible velocity-size relationship between the members of asteroidal families (Cellino et al., 1999). But our model is not aimed to reproduce the actual shape of the observed families, and the above assumption can be considered more than adequate for our purposes. Finally, we also assume that the ejection is isotropic, in agreement with the results of Zappalà et al. (1996) for most asteroidal families. Following Petit and Farinella (1993), we estimate the escape velocity as:

$$v_{esc}^2 = 1.64 G \frac{4}{3} \pi \rho_{\rm PB} R_{\rm PB}^2 \tag{8}$$

where G is the gravitational constant. Only the fragments with $v_{ej} > v_{esc}$ are able to escape, with a relative velocity "at infinity" $v_\infty^2 = v_{ej}^2 - v_{esc}^2$. From $N(v_{ej})$, we obtain the correlated distribution $N(v_\infty)$, and we further assume that it has an upper cutoff at a speed $v_{cut} = 1000$ m s^{-1}. The distribution $N(v_\infty)$ is then decomposed in the distributions tangential to the orbit $N(v_T)$, radial $N(v_R)$, and normal $N(v_W)$. Finally, the orbital elements a, e, I of the fragments relative to the parent body are computed using Gauss equations, while for λ, ϖ, Ω we assume the same values of the parent body. It is worth recalling that, to compute Gauss equations, we need to assume the values of the true anomaly f and the argument of perihelion ω at the moment of the breakup. Following the considerations in Morbidelli et al. (1995), we choose here $f = 90°$ and $f + \omega = 45°$.

Using this model of isotropic ejection, we simulated the formation of synthetic Themis families for different values of the parameter $f_{\rm KE}$. We considered a Themis-like parent body with $\rho_{\rm PB} = 1300$ kg m^{-3} (typical of C-type bodies) and $R_{\rm PB} = 200$ km. This radius was estimated by simply adding the mass of all the presently known members of the family (1850 asteroids, as determined in RNF-I), but it is also in good agreement with the estimates of Tanga et al. (1999). The orbital elements of the parent body were taken from a numerical integration of Themis itself: $a = 3.124$ AU, $e = 0.203$, $I = 1.13°$, $\sigma \simeq 0$, $\varpi - \varpi_{\rm J} \simeq 0$ and $\Omega - \Omega_{\rm J} \simeq 0$. With these values, the parent body is at a maximum of eccentricity at the moment of the breakup. The advantage of this choice is twofold: (i) it puts the parent body in its nearest approach to the 2:1 resonance border (Morbidelli et al., 1995); (ii) the resulting osculating elements a, e, I of the fragments, obtained from Gauss equations, are equivalent to their resonant proper elements a_p, e_p, I_p (recall that all fragments will have $\sigma \simeq 0$, $\varpi \simeq \varpi_{\rm J}$ and $\Omega \simeq \Omega_{\rm J}$).

In Fig.12, the shaded histogram represents the distribution in proper a of a synthetic Themis family (2000 fragments) generated with $f_{\rm KE} = 0.01$. The outlined histogram is the actual distribution of Themis family, and the small histogram at the lower-right edge corresponds to the observed Zhongguos (see Table 3 on RNF-I). As expected, the distribution of Themis family shows a sudden cutoff at the border of the 2:1 resonance (Sx). If we extrapolate this distribution inside the resonance, the Zhongguos appear to effectively lie in the tail the distribution. On the other hand, the

synthetic family shows a very narrow distribution, and the fragments were not able to reach the border of the 2:1 resonance. The difference between the synthetic and the real family is notorious, If we assume that our model of fragmentation is essentially correct, then the rather flat distribution of the real family can be related to: (i) an already flat initial distribution after the breakup, or (ii) the subsequent dynamical dispersion of the family due to weak MMRs, Yarkovsky, etc. The former option is quite improbable, because to obtain such initial flat distribution we should consider values of $f_{\rm KE} \sim 1$ or larger. Then, we believe that the second option is the actual responsible of the presently observed distribution.

On the other hand, it is worth noting that we do not need to consider very high values of $f_{\rm KE}$ to inject asteroids in the resonance. In fact, with values as small as 0.03 some fragments are already able to reach the resonance border. The actual implications of this mechanism in the origin of the Zhongguos can be better appreciated in Fig. 13. We plot there the distribution in the space of proper elements of the ejected fragments (black dots) from three simulations, using $f_{\rm KE} = 0.01$, 0.05 and 0.10, respectively. The top panels correspond to the same simulation shown in Fig. 12. The grey dots are the actual Themis family, and the open circles are the Zhongguos. The circle indicated by an arrow is Zhongguo itself. This asteroid, together with the small cluster of 1975 SX (see Fig. 7 of RNF-I), seem to be the natural extension of Themis family inside the resonance, as Morbidelli et al. (1995) already pointed out. However, the cluster of resonant asteroids that really matters is that of 1994 UD1, located at $e_p \sim 0.27$. As we showed in RNF-I, this cluster lies in the most stable region of the 2:1 resonance, and concentrates almost 70% of the stable population. According to Fig. 13, this cluster is far from the region where the possible Themis outcomes would be eventually injected, and its origin seems unlikely to be related to the breakup of Themis. However, we cannot totally rule out this possibility because there could exist some unknown dynamical mechanism inside the 2:1 resonance able to transport the injected fragments to the region of 1994 UD1. Moreover, if we consider a very energetic impact, (bottom panels of Fig. 13), some fragments can reach the resonant space at the right side of the resonance center. Due to the symmetry of the resonant motion along the lines of $N = \text{const.}$ (Eq. 1), these fragments will be actually in the region of 1994 UD1 at the left side of the resonance center. Notwithstanding, we must recall that the value $f_{\rm KE} = 0.1$ is very much larger than that we should expect in the breakup of a typical C-type body. Then, we believe that the scenario shown in the bottom panels of Fig. 13 would never hold at all.

5. Conclusions

In this paper we have analyzed different hypothesis for the origin of the asteroids in the 2:1 resonance with Jupiter (Hecuba gap). All these hypothesis are related to the idea of the injection of asteroids in the 2:1 resonance from the neighbouring regions. We have concentrated our attention on the left side of the Hecuba gap, which accounts for a huge population of asteroids, most of them related to Themis family.

We have discussed three possible mechanisms to inject asteroids in the 2:1 resonance: (i) chaotic

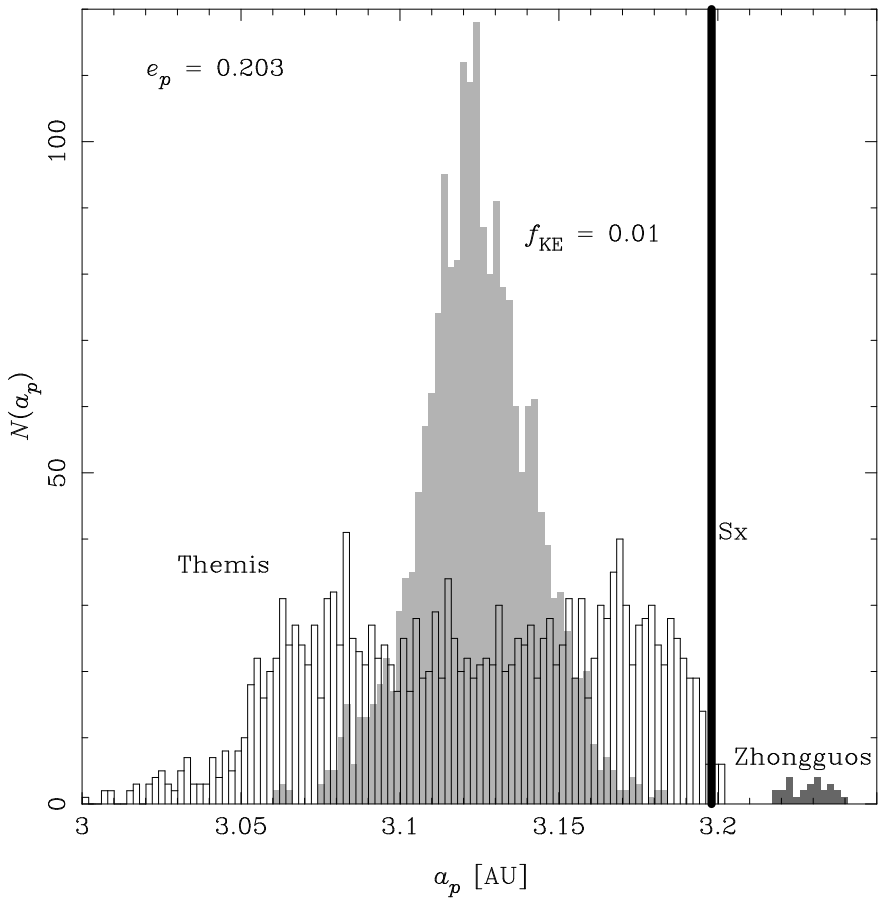

Fig. 12.— The shaded histogram represents the distribution in resonant proper semi-major axis of a synthetic Themis family, with 2000 fragments generated with our model of isotropic ejection using $f_{\rm KE} = 0.01$. The outlined histogram is the actual distribution of 1850 Themis family members. The bold vertical line indicates the location of the separatrix of the 2:1 resonance. The small histogram at the right side of the separatrix corresponds to the 61 known Zhongguos. All the histograms are projected in the plane $e_p = 0.203$.

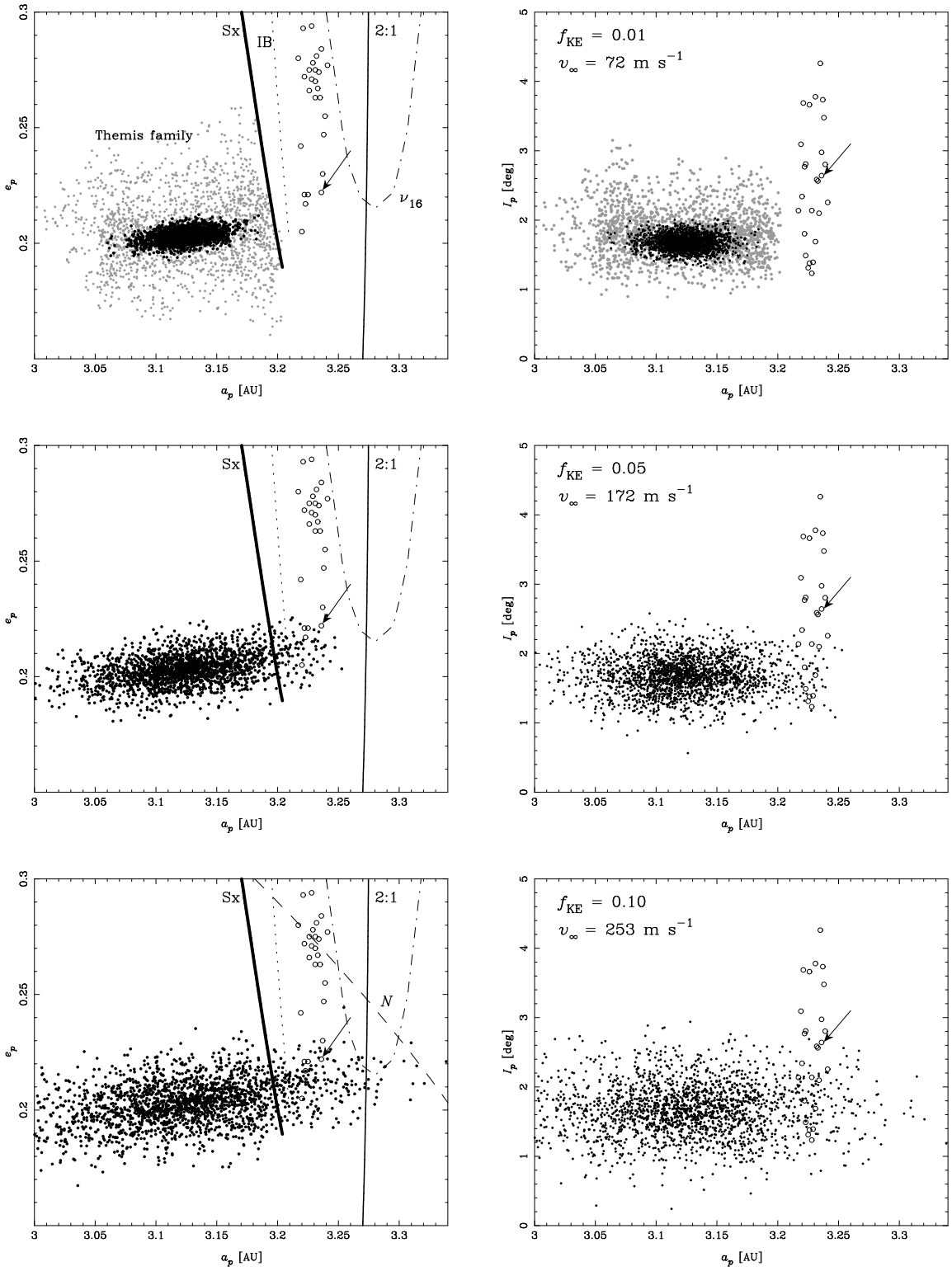
Sx
IB
2:1
Themis family
ν_{16}
f_{KE} = 0.01
v_∞ = 72 m s^{-1}
f_{KE} = 0.05
v_∞ = 172 m s^{-1}
f_{KE} = 0.10
v_∞ = 253 m s^{-1}
N
a_p [AU]
e_p
I_p [deg]

Fig. 13.—

Fig. 13.— Top to bottom: Three different simulations of the breakup of a Themis-like parent body, using different values of $f_{\rm KE}$. The black dots represent the distribution of the fragments in the space of resonant proper a, e (left) and $a.I$ (right).We generated 2000 fragments in each simulation. The average value of v_∞ is indicated in each case. The open circles are the stable resonant asteroids. The asteroid indicated by an arrow is (3789) Zhongguo. The cluster of resonant asteroids at $e_p \sim 0.27$ is the group of 1994 UD1 (see RNF-I). The gray dots in the top panels correspond to the actual Themis family. We also show the location of the resonance center (full thin line), separatrix (bold line), instability border (dotted line marked IB) and ν_{16} resonance (dotted-dashed line). In the lower-left panel, we also plot the curve of $N = \text{const.}$ (dashed line) that passes through the cluster of 1994 UD1. Recall that the motion of the resonant asteroids is symmetric with respect to the center of the resonance along this curve.

diffusion in the neighborhood of the resonance, (ii) capture due to migration of the resonance, and (iii) breakup of a Themis-like asteroid.

We have found that the dynamics at the left neighborhood of the resonance is dominated by several weak mean motion resonances, most of them involving the orbital periods of Jupiter and Saturn simultaneously. Asteroids captured in these resonances have their eccentricities excited and can reach the border of the 2:1 resonance, being then injected. This mechanism proved to be efficient over time scales of some 100 Myr, but only for asteroids that are close to the resonance border. On the other hand, the overlap of weak mean motion resonances at high eccentricities ($e > 0.35$) allows asteroids to randomly walk over large intervals of semi-major axis (~ 0.1 AU). This overlap could help to inject objects in the 2:1 resonance in an even shorter time scale (some 10 Myr).

The particles injected by these mechanisms arrive to the most unstable region of the resonant phase space, and do not survive in the resonance for more than 10 Myr, at most. Then, these mechanisms provides a flux that could help to keep the population of unstable resonant asteroids in a steady state. But it cannot account for the origin of marginally unstable (Griquas) and stable (Zhongguos) populations.

We have also discussed the possible role of Yarkovsky effect and mutual scattering by main belt asteroids in enhancing the flux of injected asteroids. For bodies larger than 5 km, Yarkovsky effect accounts for a net drift in semi-major axis of about 1/200 AU per Byr or less. Then, Yarkovsky effect can contribute to the flux of unstable resonant asteroids, but the provided drift is not enough to inject objects in the most stable places of the resonant phase space. The main constraint is related to the huge excitation of the inclinations occuring when the asteroids cross the resonance border, which is not compatible with the rather low inclinations of the observed Zhongguos. Similar considerations hold for the effects of mutual scattering.

We have investigated the possibility of resonant capture due to migration of the 2:1 resonance. If planetary migration happened during the early history of the Solar System, it caused the decay of Jupiter's semi-major axis by some 0.2 AU, with the consequent drift of the 2:1 resonance inwards.

According to our simulations, this drift could favor the capture of low-eccentricity non resonant asteroids by the 2:1 resonance. We simulated an exponential migration with a charateristic time scale of 2 Myr, and found evidence that such mechanism could create a primordial population of resonant asteroids, with dynamical properties compatible with the observed Zhongguos. However, our results need to be confirmed by more detailed studies, using more reliable models of planetary migration.

Finally, we have discussed the origin of the 2:1 resonant asteroids in the framework of the breakup that originated Themis family. We simulated a fragmentation of a Themis-like parent body using a simple model where the ejection velocity is assumed to be independent of the fragments' masses. We have found that, for small values of the anelasticity parameter $f_{\rm KE}$, typical of C-type bodies, it is not possible to inject fragments into the 2:1 resonance. For larger values, the injection is possible, but the fragments arrive to a region of the resonant phase space which is not compatible with the presently observed distribution of Zhongguos. Although we cannot rule out this mechanism of injection, a relation between the breakup of Themis and the origin of Zhongguos seems unlikely.

F. Roig wish to thank the São Paulo State Science Foundation (FAPESP) for giving financial support to this work through PhD scholarship 97/5806-9. The Department of Space Studies of the Southwest Research Institute at Boulder, Colorado, is highly acknowledge for hosting the four month visit of F. Roig during the final stages of this work. Fruitful discussions with W. Bottke, A. Morbidelli and R. Gomes helped to improve the contents of this paper, and are highly appreciated.

REFERENCES

Benz, W., and Asphaug, E.: 1999. Catastrophic disruptions revisited. *Icarus* **142**, 5–20.

Bretagnon, P.: 1982. Théorie du mouvements de l'ensemble des planètes, Solution VSOP82. *Astron. Astrophys.* **114**, 278–288.

Carruba, V., Burns, J., Bottke, W., and Morbidelli, A.: 2000. Asteroid mobility due to encounters with Ceres, Vesta, Pallas: Monte Carlo codes *vs.* direct numerical integrations. *DPS Meeting #32*, 14.06

Cellino, A., Michel, P., Tanga, P., Zappalá, V., Paolicchi, P., and Dell'Oro, A.: 1999. The velocity-size relationship for members of asteroid families and implications for the physics of catastrophic collisions. *Icarus* **141**, 79–95.

Farinella, P., and Vokrouhlický, D.: 1999. Semi-major axis mobility of asteroidal fragments. *Sci.* **283**, 1507–1510.

Fernández, J.A., and Ip, W.H.: 1984. Some dynamical aspects of the accretion of Uranus and Neptune. The exchange of orbital angular momentum with planetesimals. *Icarus* **58**, 109–120.

Fernández, J.A., and Ip, W.H.: 1996. Orbital expansion and resonant trapping during the late accretion stages of the outer planets. *Planet. Space Sci.* **44**, 431–439.

Ferraz-Mello, S.: 1994. Dynamics of the asteroidal 2/1 resonance. *Astron. J.* **108**, 2330–2337.

Ferraz-Mello, S., Michtchenko, T.A., and Roig, F.: 1998a. The determinant role of Jupiter's Great Inequality in the depletion of the Hecuba gap. *Astron. J.* **116**, 1491–1500.

Ferraz-Mello, S., Michtchenko, T.A., Nesvorný, D., Roig, F., and Simula, A.: 1998b. The depletion of the Hecuba gap *vs.* the long lasting Hilda group. *Planet. Space Sci.* **46**, 1425–1432.

Giblin, I., Martelli, G., Farinella, P., Paolicchi, P., Di Martino, M., and Smith, P.N.: 1998. The properties of fragments from catastrophic disruption events. *Icarus* **134**, 77–112.

Gomes, R.: 1995. The effect of non-conservative forces on resonance lock: Stability and instability. *Icarus* **115**, 47–59.

Gomes, R.: 1997a. Orbital evolution in resonance lock I. The restricted 3-body problem. *Astron. J.* **114**, 2166–2176.

Gomes, R.: 1997b. Dynamical effects of planetary migration on the primordial asteroid belt. *Astron. J.* **114**, 396–401.

Gomes, R.: 2000. Planetary migration and Plutino orbital inclinations. *Astron. J.* **120**, 2695–2707.

Greenberg, R., and Franklin, F.: 1976. Coupled librations in the motion of asteroids near the 2:1 resonance. *MNRAS* **173**, 1–8.

Hahn, J.M., and Malhotra, R.: 1999. Orbital evolution of planets embedded in a planetesimal disk. *Astron. J.* **117**, 3041–3053.

Henrard, J., Watanabe, N., and Moons, M.: 1995. A bridge between secondary and secular resonances inside the Hecuba gap. *Icarus* **115**, 336–346.

Knežević, Z., and Milani, A.: 2001. Synthetic proper elements for outer main belt asteroids. Submitted to *Cel. Mech. Dyn. Astr.*

Levison, H.F., and Duncan, M.J.: 1994. The long-term dynamical behavior of short-period comets. *Icarus* **108**, 18–36.

Levison, H.F., Dones, L., Chapman, C., Stern, S.A., Duncan, M.J., and Zahnle, K.: 2001. Could the Lunar "Late Heavy Bombardment" have been triggered by the formation of Uranus and Neptune? *Icarus* **151**, 286–306.

Liou, J.C., and Malhotra, R.: 1997. Depletion of the outer asteroid belt. *Science* **275**, 375–377.

Love, S.G., and Ahrens, T.J.: 1996. Catastrophic impacts on gravity dominated asteroids. *Icarus* **124**, 141–155.

Malhotra, R.: 1995. The origin of Pluto's orbit: Implications for the Solar System beyond Neptune. *Astron. J.* **110**, 420–429.

Michtchenko, T.A., and Ferraz-Mello, S.: 1996. Comparative study of the asteroidal motion in the 3:2 and 2:1 resonances with Jupiter II. Three-dimensional model. *Astron. Astrophys.* **310**, 1021–1035.

Michtchenko, T.A., and Ferraz-Mello, S.: 2001. Resonant structure of the outer Solar System in the neighborhood of the planets. *Astron. J.* **122**, 474–481.

Moons, M., Morbidelli, A., and Migliorini, F.: 1998. Dynamical structure of the 2/1 commensurability with Jupiter and the origin of the resonant asteroids. *Icarus* **135**, 458–468.

Morbidelli, A., and Moons, M.: 1993. Secular resonances inside mean motion commensurabilities. The 2/1 and 3/2 cases. *Icarus* **103**, 99–108.

Morbidelli, A., and Nesvorný, D.: 1999. Numerous weak mean motion resonances drive asteroids toward terrestial planets orbits. *Icarus* **139**, 295–308.

Morbidelli, A., Zappalà, V., Moons, M., Cellino, A., and Gonczi, R.: 1995. Asteroid families close to mean motion resonances: Dynamical effects and physical implications. *Icarus* **118**, 132–154.

Nesvorný, D., and Morbidelli, A.: 1998. An analytic model of three-body mean motion resonances. *Cel. Mech. Dyn. Astr.* **71**, 243–271.

Nesvorný, D., Morbidelli, A., Vokrouhlický, D., and Brož, M.: 2001. The Flora family: A case of the dynamically dispersed collisional swarm? Submitted to *Icarus*.

Petit, J.M., and Farinella, P.: 1993. Modeling the outcomes of high-velocity impacts between small solar system bodies. *Cel. Mech. Dyn. Astr.* **57**, 1–28.

Roig, F., Nesvorný, D., and Ferraz-Mello, S.: 2001. The asteroidal population in the Hecuba gap. Part I: Dynamics and size distribution of the resonant asteroids **(RNF-I)**. In preparation.

Rubincam, D.P.: 1995. Asteroid orbit evolution due to thermal drag. *J. Geophys. Res.* **100**, 1585–1594.

Tanga, P., Cellino, A., Michel, P., Zappalá, V., Paolicchi, P., and Dell'Oro, A.: 1999. On the size distribution of asteroid families: The role of geometry. *Icarus* **141**, 65–78.

Vokrouhlický, D., Milani, A., and Chesley, S.: 2000. Yarkovsky effect on small near-Earth asteroids: Mathematical formulation and examples. *Icarus* **148**, 118–138.

Zappalá, V., Cellino, A., Dell'Oro, A., Migliorini, F., and Paolicchi, P.: 1996. Reconstructing the original ejection velocity field of asteroid families. *Icarus* **124**, 156–180.